

MINERALOGY AND GEOCHEMISTRY OF PHOSPHATES AND SILICATES IN THE SAPUCAIA PEGMATITE, MINAS GERAIS, BRAZIL: GENETIC IMPLICATIONS

MAXIME BAIJOT AND FRÉDÉRIC HATERT[§]

Laboratoire de Minéralogie, B18, Université de Liège, B-4000 Liège, Belgium

SIMON PHILIPPO

*Section Minéralogie, Musée national d'histoire naturelle, Rue Münster 25, L-2160 Luxembourg,
 Grand-Duché de Luxembourg*

ABSTRACT

The Sapucaia pegmatite is located in the well-known Eastern Brazilian Pegmatitic Province (EBPP), Minas Gerais, Brazil. Detailed mapping of the pegmatite body revealed five zones, showing distinct mineral assemblages: a border zone (BZ), an external wall-zone (EWZ), an internal wall-zone (IWZ), an intermediate zone (IZ), and a quartz core (Q). Phosphate masses found in the pegmatite contains two different assemblages: assemblage I is formed under oxidizing conditions, and assemblage II is formed under less strongly oxidizing conditions. In both assemblages, triphylite is the only primary phosphate, and several secondary species are produced by its alteration. In association I, three main transformation stages are observed: (i) the progressive oxidation of triphylite accompanied by the leaching of Li leads to the successive crystallization of ferrisicklerite and heterosite; (ii) a hydration stage transforms triphylite into hureaulite, barbosolite, and tavorite, and (iii) a final stage, corresponding to meteoric alteration, the latest highly hydrated phosphate and oxide species. In assemblage I, ferrisicklerite is replaced by minerals like jahnsite *s.l.* and frondelite *s.l.* during the hydration stage, and in both assemblages, a second generation of Mn-rich triphylite (triphylite II) is observed. Two unusual petrographic textures were also observed, showing reactions between triphylite and albite to form montebrasite and garnet rims. These textures formed during the albitization stage, and correspond to the reactions triphylite + albite → ferrisicklerite + montebrasite + quartz, and triphylite + albite → almandine + quartz, respectively. Finally, the geochemical trends in phosphates and silicates indicate that Sapucaia is a weakly fractionated and geochemically primitive LCT-type pegmatite. The degree of differentiation of the pegmatite increases from the border to the core, as shown by a decrease of Fe/(Fe + Mn) in olivine-type phosphates, which decreases from 0.75 in the IWZ, to 0.71 in the IZ. Muscovite and tourmaline chemical compositions also show evidence of increasing degree of differentiation; for example, the Ga and Nb contents of muscovite increases from 57 and 49 ppm in the IWZ, to 86 and 80 ppm in the IZ, respectively.

Keywords: Fe–Mn phosphates, petrography, geochemistry, Sapucaia pegmatite, Minas Gerais, Brazil.

SOMMAIRE

La pegmatite de Sapucaia se trouve dans la province pegmatitique brésilienne est (EBPP), Minas Gerais, Brésil. Une cartographie détaillée de la pegmatite nous a permis d'identifier cinq zones principales correspondant à des paragenèses distinctes: une zone de bordure (BZ), une zone de mur externe (EWZ), une zone de mur interne (IWZ), une zone intermédiaire (IZ) et un cœur de quartz (Q). Les phosphates présents dans la pegmatite montrent deux paragenèses distinctes: la paragenèse I qui s'est formée sous des conditions oxydantes, et la paragenèse II qui a cristallisé sous des conditions plus réductrices. Dans les deux paragenèses, la triphylite est le seul phosphate primaire, et de nombreuses espèces secondaires se forment suite à son altération. Dans la paragenèse I, trois étapes principales de remplacement sont observées: (i) l'oxydation progressive de la triphylite et le lessivage du lithium, responsable de la cristallisation successive de la ferrisicklerite puis de l'hétérosite; (ii) une étape d'hydratation qui transforme la triphylite en hureaulite, barbosolite et tavorite, et (iii) une dernière étape correspondant à l'altération météorique, qui produit des phosphates hydratés tardifs et des oxydes. Dans la paragenèse I, la ferrisicklerite est remplacée par des minéraux comme la jahnsite *s.l.* et la frondélite *s.l.* pendant l'étape d'hydratation, et dans les deux types de paragenèse, une seconde génération de triphylite riche en Mn (triphylite II) est observée. Deux textures pétrographiques remarquables ont également été mises en évidence dans ce travail. Elles montrent des réactions entre la triphylite et l'albite, qui conduisent à la formation de couronnes de montebrasite ou de grenat. Ces textures apparaissent durant l'étape d'albitisation et

[§] E-mail address: fhatert@ulg.ac.be

correspondent respectivement aux réactions triphylite + albite \rightarrow ferrisicklerite + montebrasite + quartz, et triphylite + albite \rightarrow almandin + quartz. Finalement, les tendances géochimiques des phosphates et des silicates indiquent que Sapucaia est une pegmatite de type LCT faiblement différenciée et géochimiquement primitive. Le degré de différenciation de la pegmatite augmente des bordures vers le centre, comme le montre la diminution du rapport Fe/(Fe + Mn) dans les phosphates à structure olivine, qui varie de 0,75 dans la IWZ à 0,71 dans la IZ. Les compositions chimiques de la muscovite et la tourmaline suivent des tendances géochimiques similaires, comme le montrent par exemple les teneurs en Ga et Nb de la muscovite, qui évoluent de 57 et 49 ppm dans la IWZ, à 86 et 80 ppm dans la IZ, respectivement.

Mots-clés: phosphates Fe–Mn, pétrographie, géochimie, pegmatite de Sapucaia, Minas Gerais, Brésil.

INTRODUCTION

One of the most important pegmatite provinces in the world, the Eastern Brazilian Pegmatite Province (EBPP), is located at the east side of the São Francisco craton, mainly in the state of Minas Gerais, in Brazil. It encompasses also the states of Bahia, Espírito Santo and Rio de Janeiro (Paiva 1946, Putzer 1976, Correia Neves *et al.* 1986). In September 2008 and in July 2010, we visited several pegmatites located in the Conselheiro Pena district, between Galiléia and Mendes Pimentel (Fig. 1), in order to investigate the mineralogy and petrography of phosphate minerals, as well as their textural relationships with the associated silicates.

Among these pegmatites, the Sapucaia pegmatite was selected for detailed sampling. This pegmatite, discovered in the 1920s, was initially mined for beryl and muscovite (Pecora *et al.* 1950, Cassedanne & Baptista 1999), and is famous for its complex phosphate mineral assemblages (Lindberg & Pecora 1958, Hirson 1965, Farias 1976, Svisero 1976, Moore & Ito 1978, Cassedanne & Cassedanne 1985, Horvath & Atencio 1998, Bilal *et al.* 1998, Cassedanne & Baptista 1999), from which nine new phosphate mineral species were first discovered and described: frondelite (Lindberg 1949), faheyite (Lindberg & Murata 1952, 1953), moraesite (Lindberg *et al.* 1953), “avelinoite”, which corresponds to cyrilovite (Lindberg & Pecora 1954a, Lindberg 1957), barbosalite, tavorite (Lindberg & Pecora 1954b, 1955), lipscombite (Lindberg 1962), arrojadite (PbFe) (Chopin *et al.* 2006) and ruifrancoite (Atencio *et al.* 2007).

The discovery of these new mineral species led to a good knowledge of the mineralogy at Sapucaia pegmatite. However, phosphate mineral assemblages were never correlated with the different zones of the pegmatite, and only a general description of that pegmatite body can be found in the literature (Lindberg & Pecora 1958, Cassedanne & Baptista 1999). Moreover, weathering led to flooding of some excavations and serious landslides, which now cover a large part of the quarry, and consequently decreased chances of discovering phosphate minerals at Sapucaia.

The aims of the present paper are (i) to describe the mineral assemblages found in the various zones of the pegmatite, (ii) to investigate in detail the petro-

graphic relationships among phosphates as well as their chemical variation, in order to better understand the transformation sequences that affected these minerals, and (iii) to document the geochemical evolution of the phosphate minerals and associated silicates in order to provide insight into the genesis of the Sapucaia pegmatite.

GEOLOGICAL SETTING AND DESCRIPTION OF THE PEGMATITE BODY

Geological setting

The Eastern Brazilian Pegmatite Province (EBPP) is divided into several districts, among which the Conselheiro Pena district (Pedrosa-Soares *et al.* 2009), which consists of a gneissic and migmatitic basement dated from Archean to Lower Proterozoic (the Procrane and Piedade complexes; Nalini *et al.* 2000). The Late Proterozoic cover consists of amphibolite-facies rocks such as sillimanite–staurolite–garnet–mica-bearing schists (Rio Doce Group), with intercalations of mica-ceous quartzites (Crenaque Group) (Nalini 1997, Nalini *et al.* 2000). Most pegmatites in the EBPP originated with one of the pre-, syn-, and post-tectonic granitoids that were emplaced during the 700–450 My Brazilian orogeny (Bilal *et al.* 2000, Morteani *et al.* 2000). Two of these intrusions cross-cut the cover and the basement rocks of the Conselheiro Pena district: the Galiléia and Urucum magmatic suites, which belong to the G1 and G2 supersuites, respectively (Pedrosa-Soares *et al.* 2001, 2011). The Galiléia granitoid (595 My) is a metaluminous suite characterized by a polydiapiric batholith, consisting mainly of granodiorites and tonalites with minor granites. These rocks are associated with the pre-collisional magmatism of the Brazilian orogeny, and have calc-alkaline affinities (Nalini *et al.* 2000, Pedrosa-Soares *et al.* 2001, 2011). The Urucum suite (582 My) is composed of four different types of rocks: a granite containing megacrysts of feldspar (Urucum facies), a medium- to coarse-grained granite (Palmital facies), a tourmaline-bearing granite, and a pegmatitic granite (Nalini 1997). These rocks generally show a peraluminous composition (S-type granite) due to the syncollisional character of the orogeny (Nalini *et al.* 2000, Pedrosa-Soares *et al.* 2001, 2011).

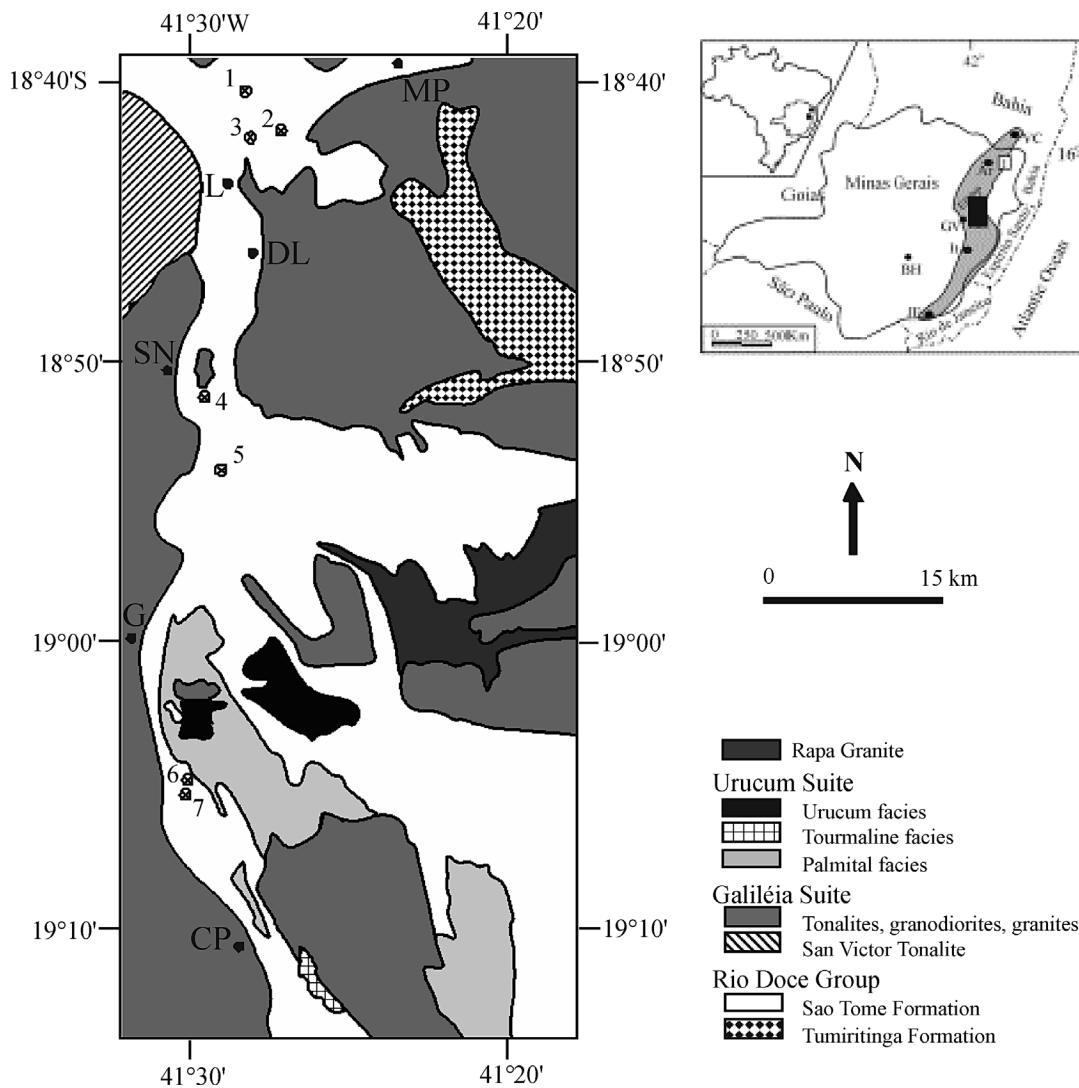


FIG. 1. Geological map of the Conselheiro Pena district (modified from Nalini *et al.* 2000, Chaves *et al.* 2005, Viana *et al.* 2007, Chaves & Scholz 2008). Localities: MP: Mendes Pimentel, L: Linópolis, DL: Divino das Larenjeiras, SN: Sapucaia do Norte, G: Galiléia, CP: Conselheiro Pena. Investigated pegmatites: 1: Telírio, 2: Sebastião Cristino, 3: Jaime, 4: Boca Rica, 5: Sapucaia, 6: João, 7: Noa Boa Vista.

Description of the pegmatite body and sampling

The Sapucaia pegmatite is located 14 km NNE of the town of Galiléia (18°54'038''S, 41°29'061''W; Fig. 1). It has an elliptical shape, 80 m in length, 40 m in width, and 50 m in height. The pegmatite intruded in the São Tome Formation, which consists in subvertical sillimanite–staurolite–garnet–mica-bearing schists. The pegmatite is zoned (Fig. 2). A border zone (BZ) 5 cm in width, in direct contact with the host schists,

has a granular texture and consists of an alternation of dark bands containing schorl + quartz, and light bands containing quartz + albite ± greenish apatite. Muscovite is an accessory mineral in the two types of layers. The external part of the wall zone (EWZ) is characterized by K-feldspar that may show a coarse graphic texture, associated with biotite and muscovite. Muscovite is coarser than biotite, and shows a fishbone-like habit, in which the crystals can reach 20 cm in length. Accessory schorl, reaching 1 to 2 cm in length, occurs in the

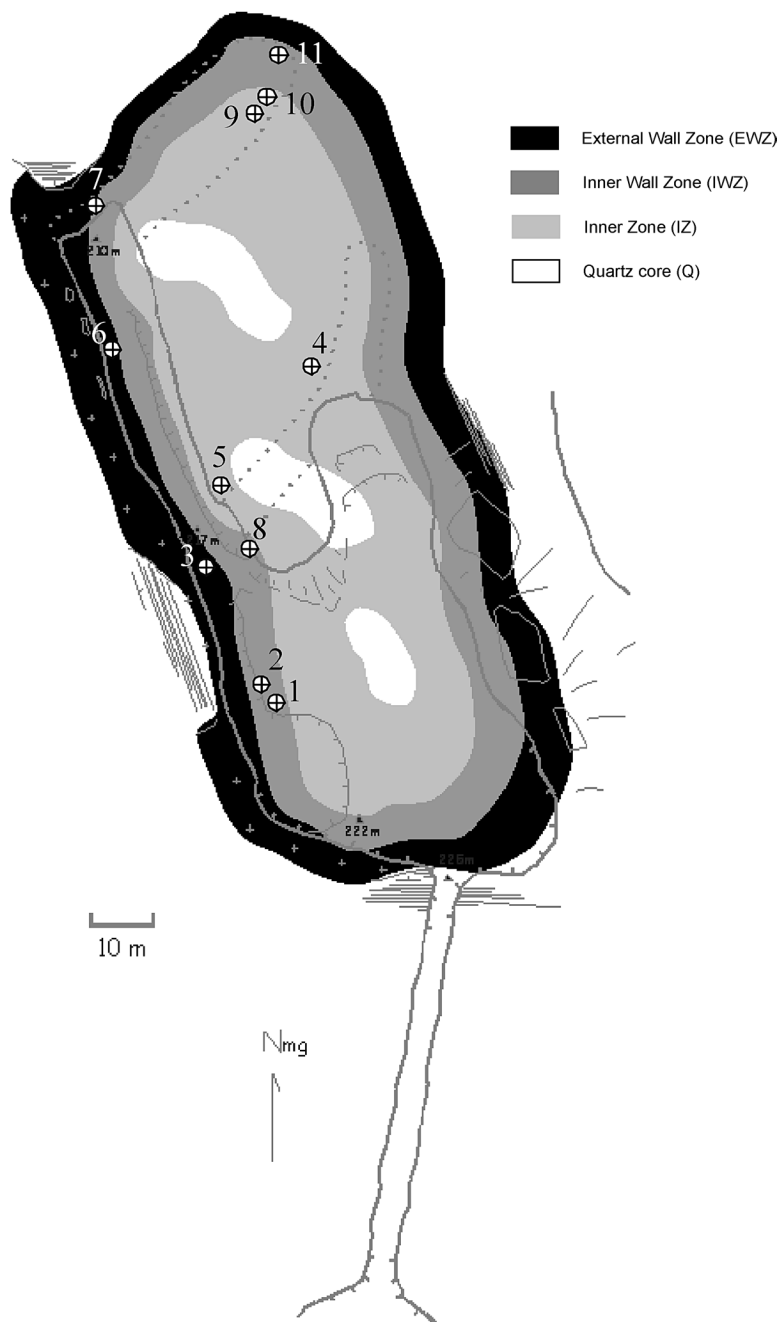


FIG. 2. Schematic map of the Sapucaia pegmatite showing the zonation and the location of the phosphate nodules (numbers). The border zone (BZ) was only observed at the entrance contact-zone and is not represented. Black zone: external wall zone (EWZ): quartz + feldspars + two micas \pm small schorl; dark grey zone: inner wall zone (IWZ): graphic K-feldspar + muscovite + schorl \pm beryl; light grey zone: inner zone (IZ): spodumene + quartz + yellow mica \pm beryl; white zone: quartz core (Q). The nodules of assemblage I are numbers 1, 2, 3, 5, 6, 8, 9, 10 and 11; the nodules of assemblage II are numbers 4 and 7. Nodules 12 and Prb-1b were not collected *in situ*, but in the mine dump, and thus are not shown on the map. The two samples contain assemblages I and II, respectively.

matrix as well as in muscovite flakes. In the internal part of the wall zone (IWZ), biotite disappears, and the assemblage is then characterized by K-feldspar (in some cases showing a graphic texture), large prisms of schorl reaching 10 cm, accessory muscovite, and beryl. In the intermediate zone (IZ), many large crystals of spodumene reaching 2 meters in length are surrounded by yellow mica in a quartz matrix. Beryl and small crystals of schorl (2 cm maximum) can be present; larger crystals of tourmaline do appear perpendicular to the spodumene crystals. Finally, there is the quartz core (Q), which locally contains a few smaller crystals of spodumene. The IWZ, IZ, and Q zones may be partially albitized.

Phosphate minerals were observed in the IWZ and IZ zones, in which they form nodular masses reaching two meters in diameter (Fig. 2). Nine masses were sampled *in situ* in the pegmatite, whereas samples 3, 6, 12, and PRB-1b were not collected in place. Assemblages of silicates occurring directly in contact with the phosphate masses were also sampled carefully. Two different types of phosphate assemblages were recognized in the field. The first assemblage (I) shows dendritic and skeletal textures involving feldspar and several secondary phosphate minerals, whereas the second assemblage (II) comprises skeletal intergrowths of fresh massive triphylite and feldspar. In this last assemblage, triphylite shows a bluish color due to a partial alteration to vivianite.

ANALYTICAL METHODS

The identification of minerals is based on the observations of thin sections under the polarizing microscope, as well as on measurements of the X-ray powder-diffraction patterns, which were acquired with a Panalytical PW3710 diffractometer (FeK α radiation, $\lambda = 1.9373 \text{ \AA}$), and with a Panalytical PW1730 diffractometer (Debye–Scherrer method, CuK α radiation, $\lambda = 1.5418 \text{ \AA}$), Université de Liège, Belgium. The unit-cell parameters were calculated using the least-squares refinement program LCLSQ 8.4 (Burnham 1991), on the basis of the *d* values corrected with Pb(NO₃)₂ as the internal standard.

Quantitative chemical analyses were performed with a Cameca SX-100 electron microprobe (Institut für Mineralogie und Kristallchemie, Universität Stuttgart, Germany) operating in the wavelength-dispersion mode, with an accelerating voltage of 15 kV, a beam current of 10 nA, and a beam diameter of 5 μm . The following standards were used: graffonite (P), wollastonite (Si, Ca), corundum (Al), periclase (Mg), sphalerite (Zn), hematite (Fe), rhodonite (Mn), albite (Na), and orthoclase (K).

Silicate minerals from each pegmatite zone were selected for X-ray fluorescence measurements with an ARL 9400XP spectrometer (Université de Liège), in order to obtain their trace-element contents (Ga, Nb, Ni,

Pb, Rb, Sr, Zn, Cr, V). All minerals were crushed manually with a hammer, isolated under a stereo microscope, and milled in an agate mortar. Concentrations of trace elements were measured on pressed powder pellets, and the data were corrected for matrix effects by Compton peak monitoring. Accuracy is estimated to be <5% for trace elements, and was evaluated using 40 international and in-house standards.

MINERALOGICAL AND PETROGRAPHIC DESCRIPTIONS

Our investigation revealed the presence of 40 minerals in the phosphate masses from Sapucaia, among which 28 phosphates, eight associated silicates, two oxides, one sulfide, and one carbonate. These minerals, as well as their chemical formulae and abundances, are given in Table 1. All minerals described below were analyzed with the electron microprobe; the complete set of chemical data are available from the Depository of Unpublished Data on the Mineralogical Association of Canada website (document Sapucaia CM50_1531).

Triphylite

Triphylite generally occurs in an albite matrix, and shows a greenish grey color that may grade to bluish where the mineral is altered to vivianite. Under the microscope, triphylite is translucent to light grey and non-pleochroic. The replacement of triphylite by hureaulite, barbosalite, and tavorite (assemblage I), as well as by vivianite (assemblage II), occurs along its two perpendicular cleavage planes, and isolates rectangles, forming a cellular texture (Fig. 3a). However, triphylite also shows a progressive oxidation to ferrisicklerite and to heterosite, following the so-called “Quensel–Mason” sequence (Quensel 1937, Mason 1941) and preserving the optical orientation of these olivine-type phosphates (Fig. 3b).

Representative compositions of triphylite from the different zones are given in Table 2, and plotted in a Fe_{tot}–Mn_{tot}–Mg triangular diagram (Fig. 4). The Fe_{tot}/(Fe_{tot} + Mn_{tot} + Mg) value increases from 0.64 for sample PRB-1b to 0.71 for sample Sap-7b, whereas the Mg/(Fe_{tot} + Mn_{tot} + Mg) value decreases from 0.19 for sample Sap-6b, to 0.02 for sample PRB-1b. The high Mg content of sample Sap-6b corresponds to 0.200 Mg atoms per formula unit (*apfu*). Higher Mg contents were already observed in triphylite samples from New Hampshire, United States, and from the Brissago pegmatite, Switzerland, in which Mg reaches 0.234 and 0.325 *apfu*, respectively (Chapman 1943, Losey *et al.* 2004, Vignola *et al.* 2008). However, most samples of triphylite in the literature have a lower Mg content (Fransolet *et al.* 1984, 1985, 1986, Keller & von Knorring 1989, Keller *et al.* 1994a, 1994b, Roda *et al.* 2004, Roda-Robles *et al.* 2010).

Ferrisicklerite and heterosite

Ferrisicklerite was found *in situ* only in sample Sap-1. In association with other phosphate minerals (mainly heterosite, jahnsite, and frondelite), it forms a dendritic texture in a quartz + albite matrix. In this hand specimen, relics of triphylite are clearly visible. Fresh ferrisicklerite displays its typical reddish brown color in hand specimens, but under the polarizing microscope, the mineral is slightly pleochroic, with absorption colors varying from deep orange to light orange. Ferrisicklerite

replaces triphylite (Fig. 3b), but is also replaced by heterosite (Fig. 3d); the optical orientation is preserved during this oxidation process. Ferrisicklerite is locally replaced along cleavage planes by jahnsite-group minerals (Figs. 3c, d), or by fibroradial crystals of frondelite (Figs. 5a, b, d).

In sample Sap-12d, a ferrisicklerite grain associated with orange hureaulite shows color variations from yellow brown to greenish brown (Fig. 3b). Such samples were already described by Fransolet *et al.* (1986), who suggested that a small amount of Fe²⁺ or

TABLE 1. FORMULA AND RELATIVE ABUNDANCE OF MINERALS FROM THE TWO PHOSPHATE ASSOCIATIONS, SAPUCAIA, MINAS GERAIS, BRAZIL

Mineral name	Formula	Abundance	
		Assoc. I	Assoc. II
Primary phosphates			
Triphylite	Li(Fe ²⁺ , Mn ²⁺)PO ₄	x	xxx
Secondary phosphates			
Ferrisicklerite	Li _{1-x} (Fe ³⁺ , Mn ²⁺)PO ₄	xx	o
Heterosite	(Fe ³⁺ , Mn ³⁺)PO ₄	xx	o
Jahnsite-(MnMg)	MnMn ²⁺ Mg ₂ Fe ³⁺ ₂ (PO ₄) ₄ (OH) ₂ •8H ₂ O	xx	o
Jahnsite-(CaMnMg)	CaMn ²⁺ Mg ₂ Fe ³⁺ ₂ (PO ₄) ₄ (OH) ₂ •8H ₂ O	xx	o
Leucosphinite	KFe ³⁺ ₂ (PO ₄) ₂ (OH)•2H ₂ O	x	o
Rockbridgeite	Fe ²⁺ Fe ³⁺ ₄ (PO ₄) ₅ (OH) ₅	xx	o
Frondelite	Mn ²⁺ Fe ³⁺ ₄ (PO ₄) ₅ (OH) ₅	xxx	o
Tavorite	LiFe ³⁺ (PO ₄)(OH)	x	o
Barbosalite	Fe ²⁺ (Fe ³⁺) ₂ (PO ₄) ₂ (OH) ₂	xx	o
Lipscombite	Fe ²⁺ (Fe ³⁺) ₂ (PO ₄) ₂ (OH) ₂	x	o
Hureaulite	(Mn ²⁺) ₄ (PO ₃ OH) ₂ (PO ₄) ₂ •4H ₂ O	xx	x
Fluorapatite	Ca ₅ (PO ₄) ₃ F	xx	x
Cyrlivite	Na(Fe ³⁺) ₂ (PO ₄) ₂ (OH) ₄ •2H ₂ O	x	x
Montebrasite	LiAlPO ₄ (OH,F)	xx	xx
Vivianite	Fe ²⁺ ₃ (PO ₄) ₂ •8H ₂ O	o	xx
Eosphorite	Mn ²⁺ AlPO ₄ (OH) ₂ •H ₂ O	o	x
Variscite	AlPO ₄ •2H ₂ O	xx	o
Phosphosiderite	Fe ³⁺ PO ₄ •2H ₂ O	xx	o
Roscherite	Ca ₂ (Mn, Fe, Mg) ₃ Be ₄ (PO ₄) ₆ (OH) ₄ •6H ₂ O	x	o
Whitmoreite	Fe ²⁺ (Fe ³⁺) ₂ (PO ₄) ₂ (OH) ₂ •4H ₂ O	x	o
Fairfieldite	Ca ₂ Mn ²⁺ (PO ₄) ₂ •2H ₂ O	o	x
Messelite	Ca ₂ Fe ²⁺ (PO ₄) ₂ •2H ₂ O	o	x
Xanthoxenite	Ca ₄ (Fe ³⁺) ₂ (PO ₄) ₄ (OH) ₂ •3H ₂ O	o	x
Ludlamite	(Fe ²⁺) ₃ (PO ₄) ₂ •4H ₂ O	o	x
Metaswitzerite	(Mn ²⁺) ₃ (PO ₄) ₂ •4H ₂ O	o	x
Whiteite-(CaMnMg)	CaMnMg ₂ Al ₂ (PO ₄) ₄ (OH) ₂ •8H ₂ O	o	x
"Whiteite-(MnMnMg)"	MnMnMg ₂ Al ₂ (PO ₄) ₄ (OH) ₂ •8H ₂ O	o	x
Associated silicates, oxides and sulfides			
Albite	NaAlSi ₃ O ₈	xxx	xxx
Microcline	KAlSi ₃ O ₈	xx	xx
Quartz	SiO ₂	xx	xx
Schorl	Na(Fe ²⁺) ₃ Al ₆ (BO ₃) ₃ Si ₆ O ₁₈ (OH) ₄	xx	xx
Muscovite	KAl ₂ (Si ₂ Al)O ₁₀ (OH) ₂	x	xx
Almandine	(Fe ²⁺ , Mn) ₃ Al ₂ (SiO ₄) ₃	xx	o
Chamosite	(Fe ²⁺ , Mg, Al, Fe ³⁺) ₆ (Si, Al) ₄ O ₁₀ (OH, O) ₈	x	x
Kaolinite	Al ₂ Si ₂ O ₅ (OH) ₄	x	x
Mn- and Fe-bearing oxide	-	xx	o
Hematite	Fe ₂ O ₃	x	o
Pyrite	FeS ₂	o	x
Siderite	FeCO ₃	o	x

In quotation marks, species not approved by IMA-CNMNC. Relative abundances in the two associations: xxx: abundant, xx: less abundant, x: scarce, o: absent.

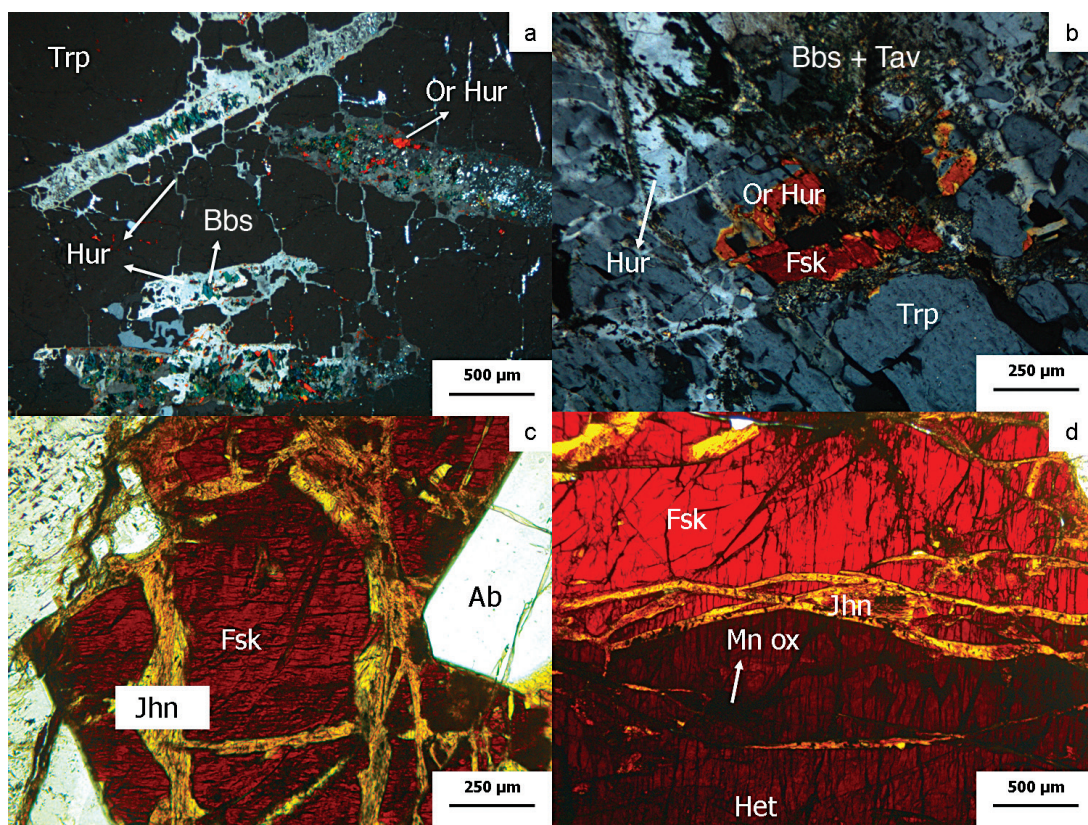


FIG. 3. a. Cellular texture in triphylite (Trp). The mineral has been replaced along its perpendicular cleavage planes by colorless hureaulite (Hur), deep green barbosalite (Bbs), and orange hureaulite (Or Hur). Assemblage I, Sap-12a, crossed polars. b. Oxidation of triphylite (Trp) into ferrisicklerite (Fsk). The optical orientation is preserved. Orange hureaulite is clearly in contact with ferrisicklerite, whereas colorless hureaulite occurs in triphylite masses associated with barbosalite and tavorite (Tav). Assemblage I, Sap-12d, crossed polars. c. Fractures filled with jahnsite *s.l.* (Jhn) cross-cut ferrisicklerite grains. Assemblage I, Sap-1, plane-polarized light. d. Ferrisicklerite oxidized to heterosite (Het) cut by fractures filled by jahnsite *s.l.* Assemblage I, Sap-1, plane-polarized light.

Mn^{3+} in the ferrisicklerite structure could explain this color variation. The presence of Mn^{3+} in the ferrisicklerite structure was recently confirmed by Hatert *et al.* (2011).

Heterosite forms dark nodular masses (the largest is $70 \times 50 \times 50$ cm in size) occurring in the dumps, which show the characteristic purple color along fractures. In thin sections, heterosite replaces ferrisicklerite, and is pleochroic with colors from deep purple to brown. Nevertheless, heterosite may appear darker owing to the presence of oxides along its cleavage planes (Fig. 3d).

The representative electron-microprobe data on ferrisicklerite and heterosite show that the Mg-Fe_{tot}-Mn_{tot} contents of triphylite, heterosite, and ferrisicklerite from the same sample do not exhibit large variations (Table 2), as these minerals are located close to each other in the Mg-Fe_{tot}-Mn_{tot} diagram (Fig. 4). Moreover,

the Mg/(Fe_{tot} + Mn_{tot} + Mg) value of minerals of the triphylite – ferrisicklerite – heterosite series shows a significant decrease, from 0.19 for samples Sap-1 and Sap-6b, to 0.02 for sample PRB-1b collected on the dumps, with intermediate values of 0.15 and 0.13 for samples Sap-7b and Sap-4, respectively (Table 2, Fig. 4). These variations are correlated with the degree of differentiation of the pegmatite body (see below).

Montebrasite

Montebrasite appears as single hypidiomorphic or euhedral crystals, which may show polysynthetic or simple twins, in an albite matrix. The proportion and the size of montebrasite crystals in the matrix may vary: the small rounded grains generally reach 10 to 50 μm in diameter, whereas the elongate grains can

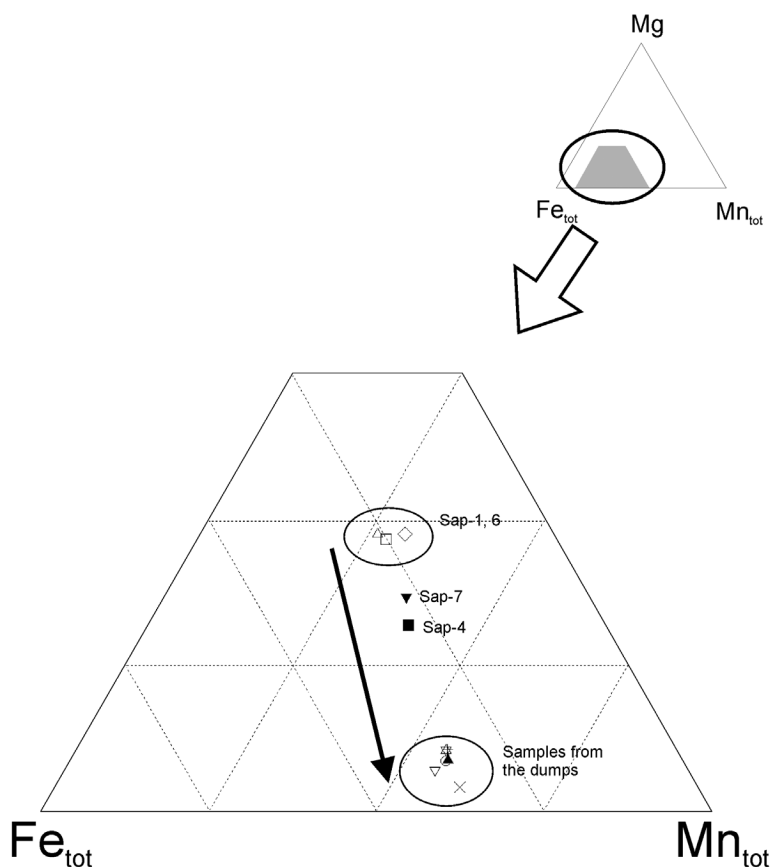


FIG. 4. The Mg–Mn_{tot}–Fe_{tot} diagram showing the average composition of minerals of the triphylite – ferrisicklerite – heterosite series. Open triangles: ferrisicklerite Sap–1; open squares: heterosite, Sap–1; black squares: triphylite, Sap–4; open diamonds: triphylite, Sap–6b; reverse black triangles: triphylite, Sap–7b; reverse open triangles: triphylite, Sap–12a; black triangles: triphylite, Sap–12d; open circles: ferrisicklerite, Sap–12d; stars: ferrisicklerite, Sap–12e; vertical crosses: heterosite, Sap–12e; diagonal crosses: triphylite, Prb–1b.

reach 1 mm in length (Sap–3) and are very abundant, up to 50% in some areas. In a skeletal texture, similar to the “lantern-like” texture described by Keller (1988), frondelite grains are separated by an intimate microcrystalline intergrowth of montebrasite + quartz (Figs. 5a, d); larger hypidiomorphic crystals of montebrasite are common in this mixture (Fig. 5a).

Fluorapatite

Fluorapatite is relatively widespread in assemblage I, where it forms an intergrowth with garnet and with associated frondelite. In sample Sap–5b, fluorapatite forms a very thin rim between frondelite and a matrix constituted by albite, quartz, and accessory microcline.

In assemblage II, fluorapatite generally occurs as minute isolated grains associated with muscovite in an albite + quartz matrix, except in sample Sap–12b, where it forms a small single crystal intimately associated with a montebrasite + quartz assemblage. A large crystal of fluorapatite, reaching 2 mm in length, has also been observed directly in contact with a large muscovite flake in sample Sap–9. The electron-microprobe analyses indicate MnO contents reaching *ca.* 2–7 wt.% in fluorapatite associated with almandine, 2 wt.% in fluorapatite occurring in the quartz + albite and quartz + montebrasite assemblages, and <1 wt.% in the fluorapatite rim associated with frondelite. Semiquantitative determinations of the fluorine contents confirm that these phosphates correspond to fluorapatite.

Minerals of the rockbridgeite–frondelite series

In hand specimens, minerals of the rockbridgeite–frondelite series appear as fibroradial crystals with a red, brown, or bottle-green color, or form small deep greenish botryoidal masses occurring in cavities. Under the polarizing microscope, the unaltered mineral forms fans of fibrous radiating crystals showing light orange to deep orange or greenish brown to deep orange colors (Figs. 5a, b, c). Some grains of frondelite–rockbridgeite clearly appear as spheroidal masses, generally larger than 50 μm in diameter, which are stacked upon each other (Fig. 5c). These botryoidal spheres generally appear on cracks and in cavities; some of them can

lose the intense pleochroism and become almost opaque (Fig. 5c).

The variations of pleochroic colors in minerals of the rockbridgeite–frondelite series are generally correlated with variations in chemical composition, as for example in sample Sap–5a, where red frondelite contains *ca.* 10–13 wt.% MnO, whereas greenish frondelite contains lower amounts of manganese, reaching *ca.* 6–7 wt.% MnO. However, in sample Sap–2, the same color variations are observed without any significant change in the manganese content; these variations are thus certainly correlated with changes in the oxidation state of iron and manganese (Table 3). Fransolet (1976) also observed that minerals of the rockbridgeite–frondelite series

TABLE 2. CHEMICAL COMPOSITION OF TRIPHYLITE, FERRISICKLERITE AND HETEROSITE FROM SAPUCAIA, MINAS GERAIS, BRAZIL

<i>n</i>	Trp	Trp	Trp	Trp	Trp	Trp	Fsk	Fsk	Het	Fsk	Het
	PRB- 1b (12)	Sap- 4 (10)	Sap- 6B (8)	Sap- 7B (7)	Sap- 12a (7)	Sap- 12d (6)	Sap- 12d (5)	Sap- 12e (4)	Sap- 12e (8)	Sap- 1 (8)	Sap- 1 (15)
SiO ₂ wt.%	–	0.31	0.43	0.17	0.02	0.04	0.06	0.06	0.06	0.72	0.48
P ₂ O ₅	46.39	46.57	45.91	45.58	46.94	46.56	46.78	46.42	47.77	47.54	48.12
Al ₂ O ₃	0.00	0.02	0.00	0.00	0.00	0.00	0.00	0.00	0.00	0.01	0.02
Fe ₂ O ₃ *	–	–	–	–	–	–	34.50	34.43	34.82	33.84	33.29
FeO*	28.86	29.28	28.89	29.30	30.22	30.52	–	–	–	–	–
MgO	0.49	3.41	5.27	3.98	0.72	0.93	0.92	1.13	1.17	5.40	5.25
Mn ₂ O ₃ *	–	–	–	–	–	–	–	–	16.33	–	11.85
MnO*	15.92	11.94	10.76	11.60	14.72	15.33	15.51	15.40	1.04	10.22	–
ZnO	0.00	0.07	0.05	0.09	0.07	0.10	0.15	0.11	0.19	0.09	0.07
CaO	0.04	0.03	0.02	0.02	0.06	0.06	0.05	0.11	0.05	0.21	0.19
Na ₂ O	0.01	0.01	0.00	0.00	0.00	0.00	–	0.03	0.00	0.01	0.00
Li ₂ O*	10.19	9.91	8.94	8.90	10.31	9.53	2.94	2.60	–	3.27	1.39
K ₂ O	0.00	0.00	0.00	0.00	0.01	0.00	0.01	0.01	0.00	0.02	0.04
Total	101.90	101.55	100.27	99.64	103.07	103.07	100.91	100.29	101.44	101.31	100.70
Si <i>apfu</i>	–	0.008	0.011	0.004	0.001	0.001	0.002	0.002	0.001	0.018	0.012
P	1.000	0.992	0.989	0.996	0.999	0.999	0.998	0.998	0.999	0.982	0.988
Al	0.000	0.001	0.000	0.000	0.000	0.000	0.000	0.000	0.000	0.000	0.001
Fe ³⁺	–	–	–	–	–	–	0.655	0.658	0.647	0.622	0.608
Fe ²⁺	0.615	0.616	0.615	0.632	0.636	0.647	–	–	–	–	–
Mg	0.018	0.128	0.200	0.153	0.027	0.035	0.035	0.043	0.043	0.197	0.190
Mn ³⁺	–	–	–	–	–	–	–	–	0.307	–	0.219
Mn ²⁺	0.343	0.255	0.232	0.254	0.314	0.329	0.331	0.331	0.022	0.211	–
Zn	0.000	0.001	0.001	0.002	0.001	0.002	0.003	0.002	0.003	0.002	0.001
Ca	0.001	0.001	0.001	0.000	0.002	0.002	0.001	0.003	0.001	0.005	0.005
Na	0.001	0.000	0.000	0.000	0.000	0.000	0.000	0.002	0.000	0.000	0.000
Li	1.044	1.004	0.915	0.923	1.043	0.972	0.298	0.265	–	0.321	0.135
K	0.000	0.000	0.000	0.000	0.000	0.000	0.000	0.000	0.000	0.001	0.001
ΣM	2.022	2.023	1.964	1.964	2.023	1.987	1.323	1.304	1.023	1.359	1.159
Fe _{tot} /(Fe _{tot} + Mn _{tot} +Mg)	0.629	0.617	0.587	0.609	0.651	0.640	0.641	0.639	0.635	0.604	0.598
Mg/(Fe _{tot} + Mn _{tot} +Mg)	0.019	0.128	0.191	0.147	0.028	0.035	0.034	0.043	0.042	0.191	0.187
Mn _{tot} /(Fe _{tot} + Mn _{tot} +Mg)	0.352	0.255	0.222	0.244	0.321	0.325	0.325	0.324	0.323	0.205	0.215

The compositions were acquired by electron-microprobe analysis. The number of cations was calculated on the basis of 1(P + Si) per formula unit; * In triphylite, all Fe is assumed to be ferrous, and Li was calculated to maintain charge balance. In ferrisicklerite and heterosite, all Fe is assumed to be ferric, and Li, Mn²⁺ and Mn³⁺ were calculated to maintain charge balance. *n*: number of analyses; –: not determined. Symbols used: Fsk: ferrisicklerite, Het: heterosite, Trp: triphylite.

progressively lose their intense pleochroism during oxidation, thus confirming this hypothesis.

Calculations of electron-microprobe data for minerals of the rockbridgeite–frondelite series commonly show an excess of negative charges, compared to the charges required by the ideal formula, $(\text{Fe}, \text{Mn})^{2+}\text{Fe}^{3+}_4(\text{PO}_4)_3(\text{OH})_5$. This excess can be explained by an auto-oxidation process according to the mechanism of substitution $\text{Fe}^{2+} + \text{OH}^- \rightarrow \text{Fe}^{3+} + \text{O}^{2-} + 1/2 \text{H}_2$ (Moore 1982, Fransolet 1976, 2007), or by the presence of significant amounts of trivalent manganese (Table 3, column 2). It is noteworthy that the presence of Mn^{3+} in rockbridgeite was confirmed by Redhammer *et al.* (2006), who explained the large Jahn–Teller distortion of the Fe2 site by the presence of Mn^{3+} at that site.

Minerals of the jahnsite group

Minerals of the jahnsite group generally occur as a thin, yellow rim or intergrowth in ferrisicklerite or in minerals of the rockbridgeite–frondelite series; they can also form small acicular crystals in cavities in feldspar and frondelite. In thin sections, yellow to yellow-brown fibrous jahnsite-group minerals replace ferrisicklerite and heterosite along their cleavage planes (Figs. 3c, d); they are in some cases intimately intergrown with fibroradial crystals of frondelite. In this case, habits of the two minerals are very similar, thus indicating replacement of frondelite by jahnsite *s.l.* Prismatic yellow jahnsite-group minerals also crystallize in cavities occurring in frondelite, and thin sections perpendicular to the prisms show the typical idiomorphic shape described by Kampf *et al.* (2008). Small acicular yellow

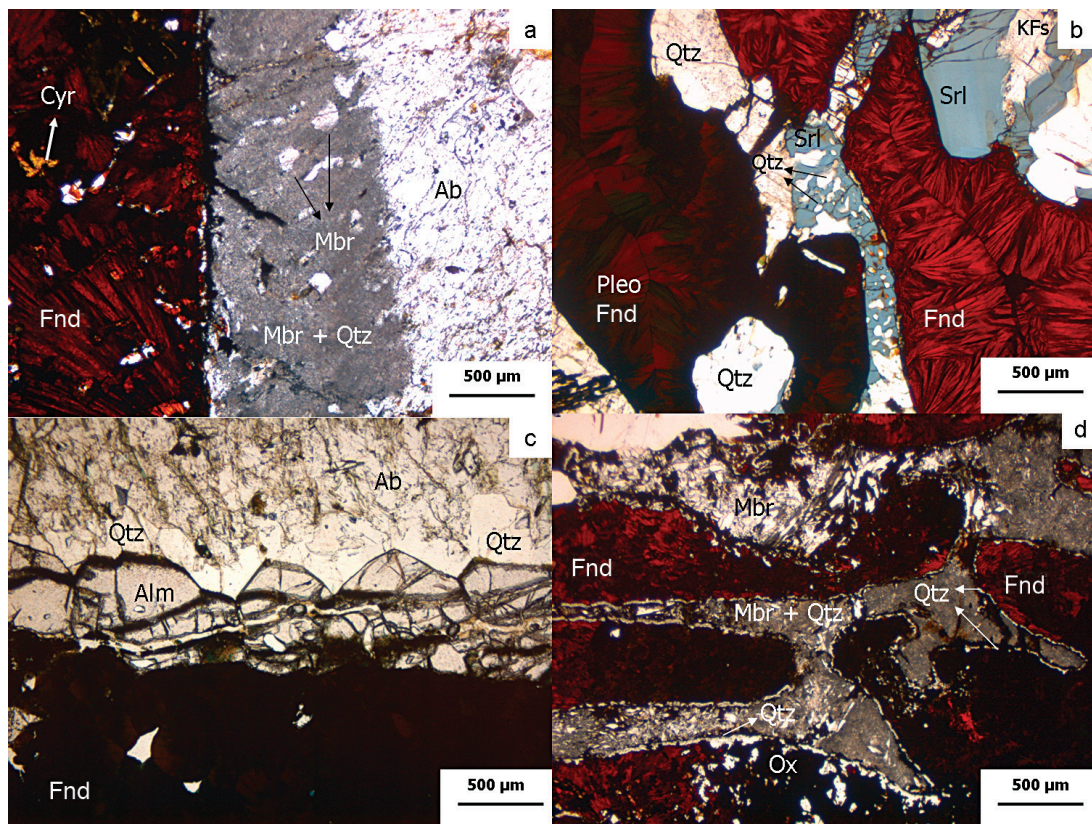


FIG. 5. a. Texture showing a rim of intimate intergrowth of quartz (Qtz) + montebrasite (Mbr), intercalated between frondelite fans (Fnd) and albite (Ab). Assemblage I, Sap-10, plane-polarized light. b. Symplectitic texture between quartz and schorl (Srl), which are directly in contact with orange frondelite and pleochroic greenish brown frondelite (Pleo Fnd). Assemblage I, Sap-3, plane-polarized light. c. Texture showing a rim of quartz + almandine (Alm), between dark spheres of frondelite and albite. Assemblage I, Sap-11, plane-polarized light. d. Skeletal texture, in which a montebrasite + quartz intergrowth surrounds large grains of frondelite. Assemblage I, Sap-3, plane-polarized light.

TABLE 3. REPRESENTATIVE COMPOSITIONS OF FRONDELITE, ROCKBRIDGEITE, JAHNSITE *s.l.*, HUREAULITE, ROSCHERITE, AND EOSPHORITE FROM SAPUCAIA, MINAS GERAIS, BRAZIL

n	Fnd	Fnd	Rck	Jhn-	Jhn-	Hur	Hur	Hur	Rsc	Eos	Eos
	a	b	c	(MnMn Mg)	(CaMn Mg)	f	g	h	l	j	k
	(62)	(57)	(31)	(39)	(12)	(4)	(6)	(24)	(3)	(3)	(5)
SiO ₂ wt. %	0.05	0.05	0.05	0.21	0.08	0.01	0.00	0.00	0.27	0.06	0.00
P ₂ O ₅	32.49	33.37	32.74	33.37	33.73	39.03	40.70	40.19	38.38	30.39	31.50
Al ₂ O ₃	0.63	0.84	0.36	1.43	1.47	0.00	0.00	0.00	0.27	21.38	21.81
Fe ₂ O ₃ *	47.04	47.96	48.18	17.07	16.44	—	1.81	—	10.43	0.03	4.48
FeO*	3.67	—	6.14	6.50	5.83	11.80	10.54	12.14	3.23	7.05	1.16
MgO	0.26	0.25	0.44	5.90	6.20	1.71	1.76	1.92	0.90	0.03	0.02
Mn ₂ O ₃ *	—	4.24	—	—	—	—	—	—	—	—	—
MnO*	7.39	5.17	4.40	12.98	12.02	34.86	33.97	35.37	12.66	23.70	24.60
ZnO	0.23	0.24	0.19	0.04	0.05	0.07	0.61	0.34	0.20	0.06	0.57
CaO	0.13	0.14	0.08	2.07	4.07	0.73	0.33	0.20	9.94	1.08	0.68
Na ₂ O	0.03	0.08	0.03	0.64	0.31	0.03	0.00	0.00	0.47	0.00	0.06
K ₂ O	0.04	0.02	0.03	0.03	0.00	0.01	0.01	0.01	0.15	0.01	0.01
BeO**	—	—	—	—	—	—	—	—	9.09	—	—
H ₂ O**	6.88	7.07	6.94	19.20	19.32	12.84	12.91	13.02	13.09	15.00	15.59
F	—	—	—	—	—	—	—	—	—	0.98	0.86
O = F	—	—	—	—	—	—	—	—	—	-0.41	-0.36
Total	98.84	99.43	99.58	99.44	99.52	101.09	102.64	103.19	99.08	99.36	100.98
Si <i>apfu</i>	0.005	0.006	0.005	0.028	0.010	0.001	0.000	0.000	0.049	0.002	0.000
P	2.995	2.994	2.995	3.972	3.990	3.999	4.000	4.000	5.951	0.998	1.000
Al	0.081	0.105	0.045	0.232	0.242	0.000	0.000	0.000	0.058	0.977	0.964
Fe ³⁺	3.853	3.830	3.916	1.808	1.73	—	0.158	—	1.437	0.001	0.126
Fe ²⁺	0.337	—	0.559	0.767	0.682	1.194	1.029	1.199	0.496	0.229	0.036
Mg	0.043	0.040	0.071	1.233	1.289	0.308	0.303	0.336	0.245	0.002	0.001
Mn ³⁺	—	0.338	—	—	—	—	—	—	—	—	—
Mn ²⁺	0.684	0.469	0.403	1.546	1.42	3.574	3.336	3.518	1.964	0.778	0.782
Zn	0.019	0.020	0.015	0.004	0.005	0.007	0.053	0.029	0.026	0.002	0.016
Ca	0.015	0.016	0.010	0.312	0.608	0.095	0.042	0.025	1.950	0.045	0.027
Na	0.006	0.017	0.005	0.174	0.085	0.006	0.000	0.000	0.167	0.000	0.004
K	0.004	0.002	0.004	0.001	0.000	0.001	0.001	0.001	0.034	0.000	0.001
Be	—	—	—	—	—	—	—	—	4.000	—	—
H	5.000	5.000	5.000	18.000	18.000	10.000	10.000	10.000	15.000	3.880	3.898
F	—	—	—	—	—	—	—	—	—	0.120	0.102

The compositions were acquired by electron-microprobe analysis. The number of cations was calculated on the basis of 3(P + Si) (frondelite *s.l.*), 4(P + Si) (jahnsite *s.l.* and hureaulite), 6(P + Si) (roscherite), and 1(P + Si) (eosporite) atoms per formula unit. * FeO, Fe₂O₃, MnO, and Mn₂O₃ were calculated to maintain the charge balance. ** H₂O and BeO were calculated according to the ideal formula of the minerals. *n*: number of analyses; —: not determined. Symbols used: Eos: eosporite, Fnd: frondelite, Hur: hureaulite, Jhn: jahnsite, Rck: rockbridgeite, Rsc: roscherite.

Samples: a) Fe-rich frondelite, b) Mn³⁺-bearing frondelite, c) Mn-rich rockbridgeite, d) jahnsite-(MnMnMg), e) jahnsite-(CaMnMg), f) colorless hureaulite, g) pleochroic Fe³⁺-bearing hureaulite, h) pleochroic hureaulite without Fe³⁺, i) roscherite, j) colorless eosporite, k) yellow eosporite.

to yellowish orange spheres of jahnsite *s.l.*, reaching 200 μm in diameter, were also observed on frondelite included in an albite matrix.

The electron-microprobe data (Table 3) show that the samples investigated herein present large compositional variations, and belong to solid solutions between two different species of the jahnsite group: jahnsite-(MnMnMg) (Chesnokov *et al.* 1989, Kampf *et al.* 2008) and jahnsite-(CaMnMg) (Moore & Araki 1974, Moore & Ito 1978, Kampf *et al.* 2008). In thin sections, the optical properties of both species are identical; they can only be distinguished under the electron microscope by different shades of grey in back-scattered electron images.

Hureaulite

In hand specimens, hureaulite appears as light pink patches, mainly associated with green barbasolite and with yellow-green tavorite. Under the microscope, colorless hureaulite invades the cleavage planes of triphylite, thus forming a cellular texture (Fig. 3a). The mineral may also be associated with barbasolite; in this case, hureaulite generally becomes slightly pleochroic, with colors from light yellow to salmon pink. This pleochroism becomes more intense close to the contact between the two minerals. Pleochroic hureaulite was also observed near a ferrisicklerite grain (Fig. 3b), in cracks cross-cutting triphylite, and in large fibroradial crystals

of frondelite. In this last sample, the colors are more intense, varying from yellowish orange to deep orange.

Electron-microprobe analyses of hureaulite show significant variations in the Fe and Mn contents. For example, in sample Sap-12d from the dumps, the slightly pleochroic hureaulite contains *ca.* 2–17 wt.% FeO, whereas the strongly pleochroic hureaulite associated with barbosolite contains *ca.* 10–26 wt.% FeO. However, these chemical variations are not systematically correlated with the color of the mineral, as shown by the average compositions in Table 3, which indicate similar FeO and MnO contents for colorless and pleochroic hureaulite. The presence of significant amounts of Fe³⁺, which can reach 0.158 *apfu* (Table 3, column 7), could explain the pinkish color of some hureaulite grains, as suggested by Fransolet (1976), but most pleochroic samples do not contain detectable Fe³⁺ (Table 3, column 8).

Barbosolite

Barbosolite generally forms deep bottle-green patches in triphylite, or occurs along the cleavage planes of this mineral, in close association with bright yellow tavorite and salmon pink hureaulite. Where the alteration is intense, grains of triphylite may be completely replaced by the assemblage barbosolite + tavorite + hureaulite, preserving the cellular texture of triphylite. Under the microscope, barbosolite shows a deep bluish green color and is in some cases almost opaque. The electron-microprobe analyses show a MnO content of 0.5 wt.%, significantly lower than the MnO content of 2 wt.% measured by Lindberg & Pecora (1955) on the type specimen.

Tavorite

Tavorite occurs as bright yellow patches on barbosolite masses, or is intimately associated with deep green barbosolite to form a rectangular lattice in triphylite. In this case, tavorite has a dull yellow-brown color. Under the microscope, tavorite is non-pleochroic and shows light greenish brown colors; in crossed polars, a polygranular texture appears. The lithium content, calculated by difference from the electron-microprobe data, shows variations between 0.93 and 1.01 *apfu*.

Cyrlilovite

Cyrlilovite appears as small powdery aggregates of crystals, generally deposited on the termination of large acicular aggregates of frondelite. In thin sections, minute yellow grains of cyrlilovite occur within cavities present in large radiating crystals of frondelite, and show slightly pleochroic colors, from yellow to deep yellow (Fig. 5a). The electron-microprobe analyses are similar to those obtained by Tarte *et al.* (1984) on cyrlilovite

from a Precambrian iron deposit in the Middleback Range, South Australia, and by Cozzupoli *et al.* (1987) on cyrlilovite from a Mn orebody in Bosa (Torre Argentina), Sardinia, Italy. The 2 wt.% Al₂O₃ observed in our sample can be explained by a solid solution between cyrlilovite and wardite, NaAl₃(PO₄)₂(OH)₄•2H₂O.

Leucophosphite

Leucophosphite forms small spots up to 1 mm in diameter in heterosite, in fibroradial crystals of frondelite, or in small cavities associated with jahnsite-group minerals. In this last case, leucophosphite shows a radiating acicular habit, indicating that it constitutes a replacement product of frondelite. Leucophosphite is non-pleochroic but lightly colored, showing tinges from light pink to light mauve, light yellow or white beige. It is noteworthy that white to beige leucophosphite contains less than 1 wt.% MnO, whereas pinkish or mauve leucophosphite contains up to 6 wt.% MnO. A small amount of Mn³⁺ could explain the pink or mauve tinges in the mineral. Under crossed polars, the mineral shows a polygranular texture that is not visible in plane-polarized light.

Phosphosiderite, metavariscite, and minerals of the strengite-variscite series

Strengite, Fe³⁺(PO₄)•2H₂O, forms a series with variscite, Al(PO₄)•2H₂O, and these two minerals have a dimorphous relation with phosphosiderite and metavariscite, respectively. The minerals only appear in assemblage I and generally occur as fibroradial spheres or patches on phosphate minerals, or as minute powdery grains in cavities present in phosphate masses. They show various colors, from milky white to light pink, violet, or blue; these colors make them easily recognizable in hand specimens. Under the microscope, strengite or phosphosiderite occurs as fibroradial spheres in frondelite and albite, or as fine-grained crystals replacing frondelite or heterosite. The colors evolve from colorless to light pink or deep violet, and the empty space between the spheres is generally filled by Mn- and Fe-bearing oxides. Strengite or phosphosiderite may also form a rim on the termination of frondelite crystals, indicating a sequence frondelite – strengite or phosphosiderite – (Mn,Fe) oxide.

The electron-microprobe analyses indicate Al contents from *ca.* 1 to 8 wt.% Al₂O₃, with the core of the spheres generally richer in Fe. It is noteworthy that deep violet strengite or phosphosiderite shows the higher MnO content, up to *ca.* 1.5–2.2 wt.% MnO, whereas the colorless samples generally contain less than 1 wt.% MnO. Variscite or metavariscite is not so abundant as strengite or phosphosiderite, shows the same habits, and exhibits a light yellow color. These minerals generally crystallize in cavities in albite or in contact with schorl.

Minerals of the roscherite group

Minerals of the roscherite group were only detected in sample Sap-5b, between two grains of microcline. The color is orange brown, and a polygranular texture appears under crossed polars. The electron-microprobe data (Table 3) indicate that the mineral investigated herein corresponds to roscherite *s.s.*, with an ideal formula $\text{Ca}_2\text{Mn}^{2+}_5\text{Be}_4(\text{PO}_4)_6(\text{OH})_4 \cdot 6\text{H}_2\text{O}$ (Rastsvetaeva *et al.* 2005, Atencio *et al.* 2007). However, this roscherite *s.s.* has a high content of Fe^{3+} , thus showing the presence of a significant substitution toward ruifrancoite, $\text{Ca}_2(\text{Fe}^{3+})_5\text{Be}_4(\text{PO}_4)_6(\text{OH})_6 \cdot 4\text{H}_2\text{O}$, which was first described in the Sapucaia pegmatite (Atencio *et al.* 2007).

Eosporite

Eosporite was observed in thin cracks in albite and microcline, or forms yellow fibroradial crystals in association with an intergrowth of montebrazite and quartz. The electron-microprobe analyses of yellow eosporite show a high Fe^{3+} content if compared to the colorless samples (Table 3). According to Fransolet (1980), an oxidation process similar to that observed in rockbridgeite could also occur in eosporite, leading to a complete solid-solution between $(\text{Mn}_{1-x}\text{Fe}^{2+}_x)\text{AlPO}_4(\text{OH})_2 \cdot \text{H}_2\text{O}$ and $(\text{Mn}_{1-x}\text{Fe}^{3+}_x)\text{AlPO}_4(\text{OH})_{2-x}\text{O}_x \cdot \text{H}_2\text{O}$. This progressive oxidation would involve an increase of absorption, with yellow tinges and then orange-brown colors as Fe^{3+} increases, respectively. The chemical data presented here confirm this observation (Table 3).

Vivianite and metavivianite

Vivianite, which gives a blue color to the hand specimens of triphylite, generally occurs along the cleavage planes of this mineral, and shows an intense pleochroism from colorless to deep blue. Where the replacement of triphylite is important, vivianite takes a polygranular habit. The chemical analyses show that vivianite from the dumps (Prb-1b) is poorer in Mn (about 3 wt.% MnO) and richer in Mg (about 8 wt.% MgO) than vivianite from Sap-4, which is relatively depleted in Mg (maximum 4 wt.% but generally under 1 wt.% MgO) and richer in Mn (9 wt.% MnO). In sample PRB-1b, a significant amount of Fe^{3+} is necessary to maintain charge balance; this oxidation results in metavivianite, $\text{Fe}^{2+}_{3-x}\text{Fe}^{3+}_x(\text{PO}_4)_2(\text{OH})_x \cdot (8-x)\text{H}_2\text{O}$.

Whitmoreite, whiteite-group minerals, metaswitzerite, fairfieldite, ludlamite, messelite, and xanthoxenite

Except for whitmoreite, which was found in association with frondelite in assemblage I, these phosphates occur exclusively in assemblage II, in association with vivianite or triphylite. Owing to their small size, they

are difficult to identify under the polarizing microscope and were only detected with the electron microprobe.

Associated silicates and other minerals

The main silicates from the different zones of the Sapucaia pegmatite are microcline, albite, quartz, muscovite, and a black tourmaline-group mineral. These silicates also occur in the two types of phosphate assemblages described above. Saccharoidal albite constituting the matrix for detritic phosphates is dominant. Schorl was observed in contact with triphylite, ferrisicklerite or frondelite, and may show an unusual symplectitic texture with quartz (Fig. 5b). In thin section, we observe a chemical zonation in tourmaline-group minerals, but the analyzed samples generally show a composition of schorl, except three separate grains that correspond to elbaite (Fig. 6, Table 4).

Elbaite was not observed in close association with phosphate minerals, but occurs as bluish elongate prisms perpendicular to a spodumene crystal. The electron-microprobe analyses of this sample (Table 4, columns 9–10) show that this elbaite is completely depleted in Mg and richer in Zn than the other tourmaline-group minerals observed in Sapucaia (Fig. 6); a chemical zonation explains the different iron contents observed in these crystals. In sample Sap-3, a strong zonation from schorl to elbaite also is observed (Fig. 6, Table 4). It is noteworthy that if we consider tourmaline from the same location in the pegmatite, schorl associated with phosphate minerals generally contains a higher amount of MgO compared to schorl from the silicate matrix (Fig. 6).

In some thin sections of assemblage I, garnet forms a rim around the skeletal texture in frondelite observed in the albite matrix (Fig. 5c). A rim of quartz showing a polygonal recrystallization texture is present between the albite matrix and garnet (Fig. 5c). Grains of garnet are commonly associated with Mn-bearing fluorapatite, and the electron-microprobe data indicate almandine with high spessartine component (Table 5). It is noteworthy that all garnet samples investigated here show a high P content, reaching 0.40 wt.% P_2O_5 (Table 5), as previously observed in many granitic rocks (Taylor & Wise 1995, Burt 1996; Taylor *et al.* 1997, Anderson *et al.* 1998, Zhang *et al.* 2001, Arima & Yamashita 1994, Breiter & Koller 2003). Many mechanisms of substitution accounting for the incorporation of P in garnet are reported by Breiter *et al.* (2005), and sample Sap-11 shows the dominant substitution $2\text{Si}^{4+} \rightarrow \text{P}^{5+} + \text{Al}^{3+}$ (Table 5). In sample Sap-2, a minor hydrogarnet component is necessary to maintain charge balance; this component is similar to that measured by infrared spectroscopy in garnet samples from the Rutherford no. 2 and Himalaya mine pegmatites (Arredondo *et al.* 2001). Chlorite-group minerals also appear in cracks within garnet, in triphylite, or in association with frondelite and jahnsite. The replacement of garnet by chlorite is

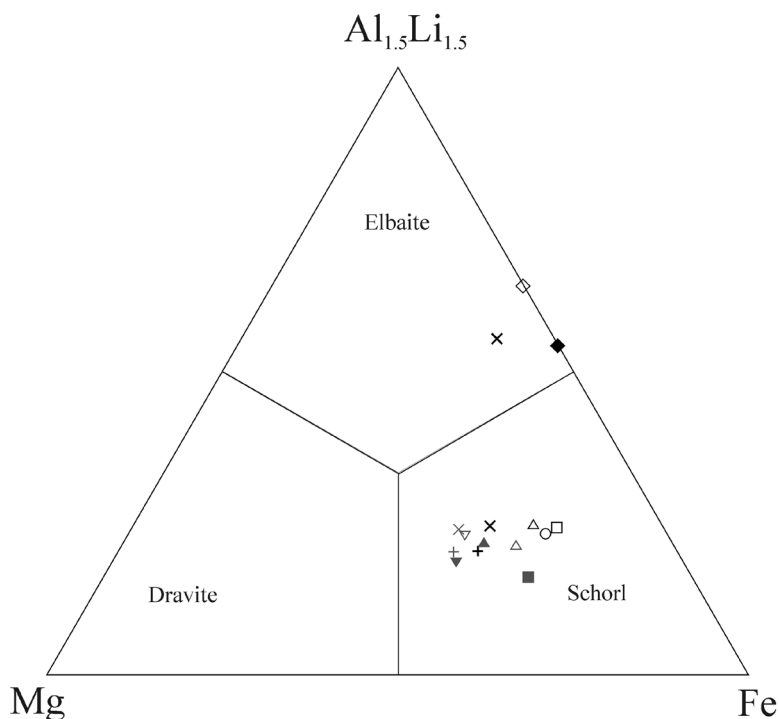


FIG. 6. The $\text{Al}_{1.5}\text{Li}_{1.5}$ -Mg-Fe diagram showing the average composition of tourmaline-group minerals occurring within phosphate masses (grey color), and found in association with enclosed silicates (black color). Vertical crosses: Sap-1; reverse open triangle: Sap-2; diagonal crosses: Sap-3 (zoned grain); open triangles: Sap-4; black triangle: Sap-5; reverse black triangle: Sap-6; black square: Sap-7; open circle: Sap-10; open square: Sap-11; open diamond: Sap comb structure (zoned grain); black diamond: Sap comb structure (zoned grain).

well known in pegmatites (Moore 1982, Vignola *et al.* 2008), and the electron-microprobe analyses (Table 5) indicate a composition of chamosite.

Muscovite directly associated with phosphates generally occurs in the albite matrix, and in some cases, it shows a symplectitic texture with quartz. Muscovite flakes in contact with triphylite masses of association II may crystallize perpendicularly to the contact, much as in a comb texture, and can be totally replaced by green chamosite. Muscovite also appears in fibroradial aggregates of frondelite in association I, where it is partially replaced by oxides. As shown by the electron-microprobe results (Table 5), muscovite from the IWZ contains a higher amount of Fe and Mg than muscovite from the IZ. However, this trend is not observed for muscovite closely associated with the phosphates. Biotite occurs only in the silicate assemblage of the EWZ, and was not observed in close association with phosphate minerals.

Finally, results of analyses of the silicates from different zones for trace elements are compiled in

Table 6; they show that schorl has a relatively high amount in Cr, Zn and Ga, as reported by Roda-Robles *et al.* (2004) on black tourmaline from the Cañada pegmatite, Salamanca, Spain. Muscovite also presents relatively high concentrations in Rb, Zn, Ga, and Nb, as other samples from the EBPP (Viana *et al.* 2007); however, these values are very low compared to those of micas from more differentiated pegmatites (Roda *et al.* 1999, Morteani *et al.* 2000, Alfonso *et al.* 2003). The K-feldspar is moderately rich in Pb, as observed for K-feldspar from the Cap de Creus pegmatite field (Alfonso *et al.* 2003), and beryl contains a relatively large amount of Cr and Zn.

Pyrite and hematite, as well as Mn- and Fe-bearing oxides, occur in the cleavage planes or cracks in triphylite and heterosite, respectively. In Assemblage I, siderite is observed in cracks in triphylite or in association with barbosalite, hureaulite, and tavorite. Kaolinite is relatively scarce, small spheres of saléeite were observed with frondelite on a smoky quartz crystal

from the quartz core, and löllingite was found between lamellae of albite.

DISCUSSION

Genetic sequence of Fe–Mn phosphates

For each type of assemblages, the textural relationship observed in thin sections and described above allow one to establish the genetic sequence of Fe–Mn-bearing phosphate minerals, which is given in Figure 7.

Triphylite was the only primary phosphate of both assemblages; nevertheless, primary fluorapatite was present in assemblage I, invariably associated with garnet. According to London *et al.* (1999), Mn-rich fluorapatite appears after the crystallization of garnet where the phosphorus content increases in the melt, but as we will see in the next paragraph, the relationships between Fe–Mn phosphates and garnet are probably more complex at Sapucaia. Triphylite crystallized shortly before the magmatic Li stage described by Ginsburg (1960), as this mineral was found in the IWZ, in which spodumene, a mineral that typically crystallizes

TABLE 4. CHEMICAL COMPOSITION OF TOURMALINE-GROUP MINERALS FROM SAPUCAIA, MINAS GERAIS, BRAZIL

n	Schorl	Schorl	Schorl	Schorl	Schorl	Elbaite	Schorl	Schorl	Elbaite	Elbaite	Schorl
	a (20)	b (9)	c (18)	d (25)	e (5)	f (7)	g (8)	h (8)	i (8)	j (5)	k (21)
SiO ₂ wt. %	36.04	35.92	35.87	35.91	36.18	36.40	36.09	35.76	35.90	36.18	35.89
P ₂ O ₅	0.02	0.02	0.01	0.02	0.01	0.02	0.01	0.00	0.01	0.02	0.01
B ₂ O ₃ *	10.57	10.55	10.59	10.60	10.75	10.95	10.69	10.63	10.78	10.87	10.64
Al ₂ O ₃	33.69	34.13	34.34	34.33	35.51	39.15	34.70	35.18	38.07	38.78	35.01
FeO	10.22	11.74	10.30	11.58	11.15	8.12	11.19	13.04	9.02	7.13	12.58
MgO	4.02	2.89	3.72	3.06	3.02	1.02	3.47	1.84	0.01	0.01	2.17
MnO	0.20	0.17	0.16	0.18	0.17	0.27	0.15	0.24	0.53	0.42	0.20
ZnO	0.08	0.10	0.09	0.11	0.14	0.08	0.11	0.18	2.23	2.07	0.16
CaO	0.06	0.06	0.05	0.06	0.06	0.07	0.05	0.04	0.02	0.08	0.05
Na ₂ O	2.16	1.90	2.07	2.09	1.95	1.95	2.14	1.90	1.85	2.36	1.93
Li ₂ O**	0.17	0.14	0.16	0.16	0.16	0.82	0.14	0.14	0.64	1.01	0.16
K ₂ O	0.05	0.03	0.04	0.04	0.03	0.02	0.04	0.04	0.02	0.03	0.04
H ₂ O*	3.65	3.55	3.57	3.66	3.64	3.67	3.60	3.61	3.54	3.50	3.59
F	–	0.20	0.18	–	0.14	0.22	0.18	0.13	0.38	0.53	0.18
O=F	–	-0.08	-0.08	–	-0.06	-0.09	-0.08	-0.05	-0.16	-0.22	-0.08
Total	100.93	101.32	101.07	101.80	102.85	102.67	102.48	102.68	102.84	102.77	102.53
T: Si apfu	5.927	5.915	5.888	5.886	5.850	5.779	5.867	5.845	5.791	5.784	5.86
P	0.002	0.002	0.001	0.003	0.002	0.003	0.002	0.000	0.002	0.003	0.001
Al	0.071	0.083	0.111	0.111	0.148	0.218	0.131	0.155	0.207	0.213	0.137
B	3.000	3.000	3.000	3.000	3.000	3.000	3.000	3.000	3.000	3.000	3.000
Z: Al	6.000	6.000	6.000	6.000	6.000	6.000	6.000	6.000	6.000	6.000	6.000
Y: Al	0.460	0.541	0.533	0.520	0.618	1.110	0.516	0.622	1.029	1.094	0.603
Mg	0.985	0.710	0.910	0.748	0.728	0.241	0.840	0.448	0.004	0.003	0.528
Fe ²⁺	1.405	1.616	1.414	1.587	1.508	1.078	1.521	1.782	1.216	0.954	1.718
Mn	0.028	0.024	0.023	0.025	0.023	0.036	0.021	0.033	0.072	0.056	0.027
Zn	0.010	0.012	0.010	0.013	0.016	0.010	0.013	0.022	0.265	0.245	0.020
Li	0.112	0.096	0.110	0.106	0.107	0.525	0.089	0.093	0.414	0.648	0.104
Σ Y	3.000	3.000	3.000	3.000	3.000	3.000	3.000	3.000	3.000	3.000	3.000
X: Ca	0.010	0.011	0.008	0.011	0.010	0.012	0.009	0.008	0.004	0.013	0.008
Na	0.690	0.607	0.659	0.664	0.610	0.601	0.674	0.603	0.579	0.731	0.611
K	0.010	0.006	0.009	0.008	0.006	0.005	0.008	0.008	0.004	0.006	0.008
□	0.290	0.376	0.324	0.317	0.374	0.382	0.309	0.381	0.413	0.250	0.373
OH	4.000	4.000	3.908	4.000	3.927	3.890	3.907	3.933	3.805	3.732	3.907
F	–	–	0.092	–	0.073	0.110	0.093	0.067	0.195	0.268	0.093

Cation numbers were calculated on the basis of 49 positive charges per formula unit, and all Fe and Mn were assumed to be divalent; * B₂O₃ and H₂O were calculated according to the ideal formula with (OH + F) = 4 apfu. ** Li was taken to be equal to the ideal sum of the Y crystallographic site minus the amount of other cations occupying those sites (Li = 3 – Y), and the calculation was iterated to self-consistency (Burns *et al.* 1994). – : not determined. n: number of analyses.

Samples: a. Mg-rich schorl, IWZ, Sap-1 and Sap-2. b. Mg-poor schorl, IWZ, Sap-1, Sap-2 and Sap-7. c. Sap-3 and Sap-6, not in place. d. IZ, Sap-4, Sap-5a and Sap-5b. e. EWZ, Sap-3. f. EWZ, Sap-3. g. IWZ, Sap-1. h. IWZ, Sap-11. i. Fe-rich elbaite, IZ, comb structure. j. Fe-poor elbaite, IZ, comb structure. k. IZ, Sap-4 and Sap-10. Samples in columns a, b, c, and d occur within the phosphate masses, whereas samples in the columns e-k occur within host silicates.

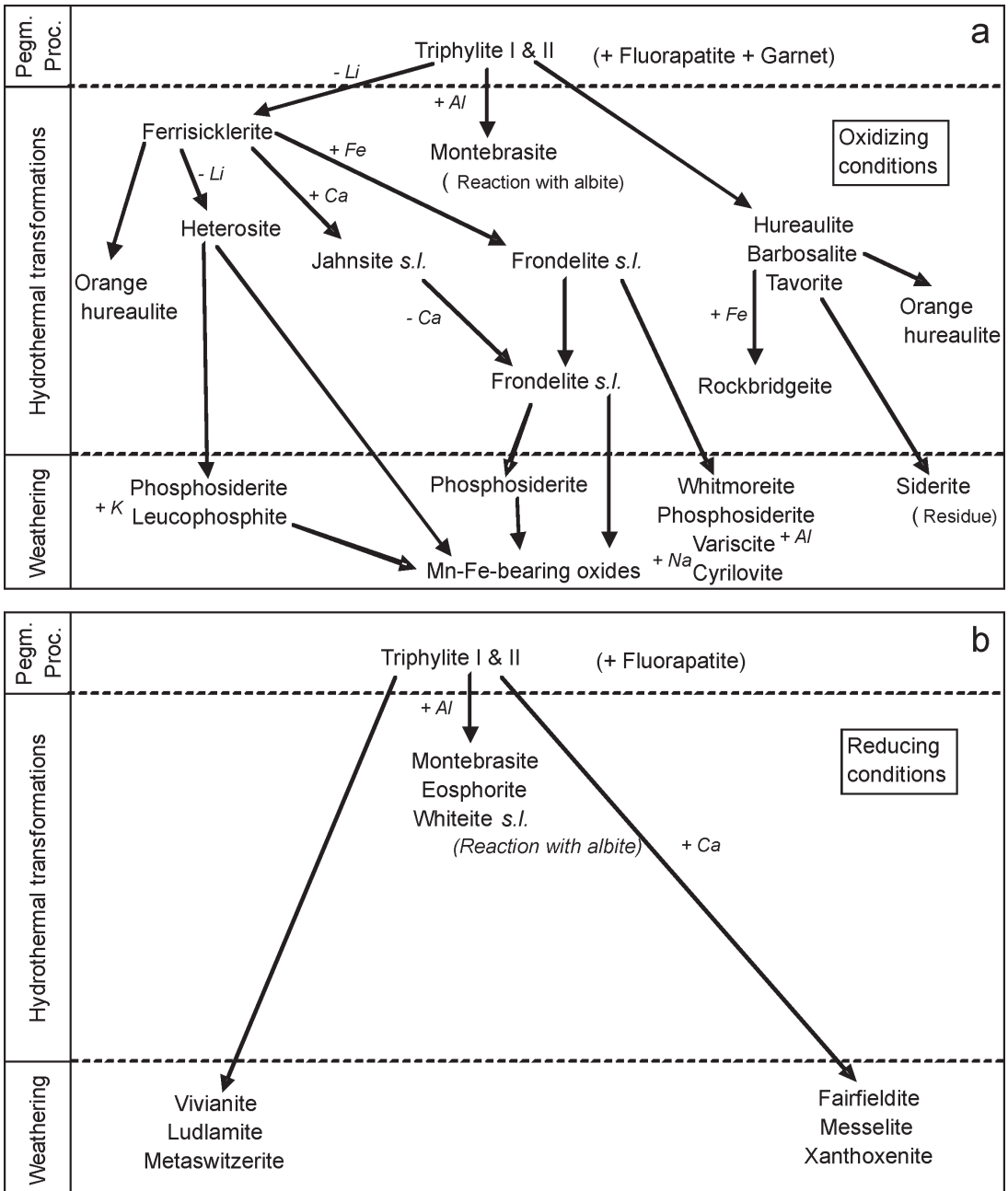


FIG. 7. Schematic representation of the alteration sequences of Fe-Mn-bearing phosphate minerals from Sapucaia pegmatite, Minas Gerais, Brazil. a. Assemblage I. b. Assemblage II.

during this Li stage, is absent. During the crystallization of triphylite in the IWZ, the activity of $(\text{PO}_4)^{3-}$, Li^+ , Fe^{2+} and Mn^{2+} was very high (Moore 1982), whereas

an increase in the activity of $(\text{SiO}_4)^{4-}$ led to the formation of spodumene associated with triphylite in the IZ.

After this magmatic Li stage, triphylite was affected by hydrothermal processes and replaced by several species under different physicochemical conditions. In assemblage I, a first stage of hydrothermal oxidation caused the replacement of triphylite by ferrisicklerite and heterosite, following the so-called “Quensel–Mason” sequence, consisting in a progressive oxidation of the metallic cations and a concomitant leaching of Li (Quensel 1937, Mason 1941). Some authors have suggested a primary origin for ferrisicklerite (Corbellá & Melgarejo 1990, Roda *et al.* 1996, 2004, Roda-Robles *et al.* 1998). In our case, even if triphylite was not found in association with ferrisicklerite systematically, other textural features confirm that ferrisicklerite crystallized from pre-existing triphylite, as discussed

by Fontan *et al.* (1976). For example, fibrous yellow jahnsite replaced ferrisicklerite along fractures (Fig. 3c); this replacement process was certainly facilitated by the volume contraction of the triphylite unit-cell due to the oxidation of Fe²⁺ to Fe³⁺ during the formation of ferrisicklerite. It is noteworthy that the Na metasomatism that generally affects triphylite to form alluaudite in many pegmatites (Fransolet *et al.* 1985, 1986, Roda *et al.* 1996, Roda-Robles *et al.* 2010), did not develop at Sapucaia; no alluaudite was observed.

In association I, the second stage of the hydrothermal transformations caused hydrated phosphate minerals to form. Consequently, triphylite was replaced by an assemblage containing colorless hureaulite, barbosalite, tavorite, and weakly hydrated phosphates.

TABLE 5. CHEMICAL COMPOSITION OF GARNET, CHLORITE, MUSCOVITE AND BIOTITE FROM SAPUCAIA, MINAS GERAIS, BRAZIL

n	Alm	Alm	Chm	Ms	Ms	Ms	Ms	Ms	Bt		
	a	b			d	e	f	g		h	
	(8)	(6)	(14)	(48)	(34)	(20)	(18)	(18)	(7)		
SiO ₂ wt. %	35.72	35.84	23.91	45.98	45.62	45.50	45.17	45.86	35.40		
P ₂ O ₅	0.40	0.38	0.11	0.08	0.05	0.04	0.08	0.03	0.04		
Al ₂ O ₃	20.56	20.51	22.36	35.25	37.97	36.02	32.48	37.99	19.64		
FeO*	22.63	22.50	34.62	1.31	0.47	1.77	3.84	0.39	19.77		
Fe ₂ O ₃ *	0.000	1.63	–	–	–	–	–	–	–		
MgO	0.54	0.70	5.61	0.54	0.06	0.42	1.14	0.03	7.86		
MnO	18.44	19.09	0.88	0.03	0.03	0.04	0.22	0.03	0.53		
ZnO	0.08	0.04	0.36	0.04	0.04	0.03	0.06	0.02	0.04		
CaO	0.25	0.27	0.04	0.02	0.00	0.02	0.02	0.03	0.00		
Na ₂ O	0.02	0.03	0.03	0.60	0.63	0.47	0.30	0.68	0.16		
K ₂ O	0.00	0.00	0.02	10.55	10.59	10.35	10.73	10.47	9.29		
H ₂ O*	0.09	0.00	10.79	4.38	4.47	4.47	4.34	4.48	3.63		
F	–	–	–	0.20	0.15	0.01	0.07	0.15	0.46		
F=O	–	–	–	-0.08	-0.06	-0.00	-0.03	-0.06	-0.20		
Total	98.73	100.99	98.73	98.90	100.02	99.14	98.42	100.10	96.62		
T: Si <i>apfu</i>	2.976	2.926	Si	2.657	Si	3.083	3.012	3.052	3.099	3.022	2.759
P	0.028	0.026	³¹ P	0.010	³¹ P	0.005	0.003	0.002	0.005	0.002	0.003
Al	0.000	0.048	²⁷ Al	1.333	²⁷ Al	0.912	0.985	0.946	0.896	0.976	1.238
Y: Al	2.019	1.926	²⁷ Al	1.595	²⁷ Al	1.874	1.970	1.901	1.729	1.974	0.566
Fe ³⁺	0.000	0.074	Fe ²⁺	3.219	Fe ²⁺	0.074	0.026	0.100	0.221	0.022	1.288
Σ Y	2.019	2.000	Mg	0.930	Mg	0.054	0.006	0.042	0.117	0.003	0.914
X: Fe ²⁺	1.577	1.537	Mn	0.083	Mn	0.002	0.002	0.002	0.013	0.001	0.035
Fe ³⁺	0.000	0.026	Zn	0.029	Zn	0.002	0.002	0.001	0.003	0.001	0.003
Mg	0.067	0.085	Ca	0.005	Σ ^{VI} X	2.006	2.006	2.046	2.083	2.001	2.806
Mn	1.302	1.320	Na	0.006	Ca	0.001	0.000	0.001	0.002	0.002	0.000
Zn	0.005	0.003	K	0.003	Na	0.078	0.081	0.061	0.027	0.087	0.024
Ca	0.022	0.024	Σ ^{VI} X	5.87	K	0.903	0.892	0.886	0.939	0.880	0.923
Na	0.003	0.004	Σ	–	Σ	0.982	0.973	0.948	0.968	0.967	0.947
K	0.000	0.000									
Σ X	2.976	2.999									
H	0.052		8.000		1.958	1.969	1.998	1.985	1.970	1.886	
F			–		0.042	0.031	0.002	0.015	0.030	0.114	

Cation numbers were calculated on the basis of eight cations (almandine), eighteen (O,OH) (chamosite), and twelve (O, OH) (muscovite, biotite) per formula unit. * Fe₂O₃ and H₂O were calculated to maintain charge balance. Symbols used: Alm: almandine, Bt: biotite, Chm: chamosite, Ms: muscovite. –: not determined. n: number of analyses.

Samples: a. Sap-2. b. Sap-11. c. Sap-1, Sap-2, Sap-3, Sap-4, Sap-5a, Sap-6a, Sap-6b, and Sap-11a. d. Sap-1, Sap-3, Sap-7, Sap-schorl, and Sap-11a. e. Sap-4, Sap-cook, Sap-8, Sap-9, and Sap-10. f. Sap-1, Sap-2, Sap-7a, Sap-7b, and Sap-11a. g. Sap-4, Sap-5b, and Sap-12b. h. Sap-8b, Sap-9, and Sap-10. i. EWZ, Sap-6. Samples in columns a, b, c, f, g, and h occur within the phosphate nodules, whereas samples in columns d, e, and i occur within the host silicates.

As discussed by several authors (Quensel 1957, Fransolet 1976, Moore & Molin-Case 1974), this replacement of primary triphylite by hureaulite and barbosalite preserves the Fe/Mn value. The electron-microprobe analyses performed on phosphates from Sapucaia confirm this assumption, as shown by sample Sap-12a, in which the average Fe/(Fe + Mn) value, 0.70, calculated considering 50% hureaulite [Fe/(Fe + Mn) = 0.41] and 50% barbosalite [Fe/(Fe + Mn) = 0.99], is in good agreement with the Fe/(Fe + Mn) ratio of parent triphylite (0.66; Table 2). In sample Sap-12d, which was affected by intense alteration, tavorite occurs in association with hureaulite and barbosalite, and the average Fe/(Fe + Mn) value was calculated considering 33% of each secondary phosphate. This average value, 0.73, also is close to the Fe/(Fe + Mn) value measured in triphylite from this sample (0.66; Table 2).

The oxidizing conditions affecting triphylite before this replacement must not be very strong, in order to avoid the oxidation of triphylite to ferrisicklerite. However, ferrisicklerite was also later affected by this hydration stage, as shown by the replacement of this mineral by jahnsite *s.l.* and frondelite *s.l.*, minerals containing OH or H₂O ligands. The frondelite spheres (Fig. 5c) certainly appear under more oxidizing conditions, as suggested by Fransolet (1976).

Finally, meteoric processes (weathering) constitute the last stage in assemblage I, during which leuco-

phosphite generally replaced heterosite, whereas other phosphates such as phosphosiderite, variscite, cyrilovite replaced frondelite. These minerals are highly hydrated and finer grained than the primary or hydrothermal species. The difference between the hydrothermal product and the meteoric species is not obvious; nevertheless, during metasomatic and hydrothermal process, the main ligands are (OH⁻) and F⁻, and the replacement of primary phases operated approximately with a conservation of volume (Moore 1982). The presence of large amounts of H₂O molecules in the atomic structure of the meteoric species generally leads to a destruction of pre-existing textures, and to a rather nodular replacement texture (Moore 1973). Finally, a superficial coating of ferric and manganic oxides replaced triphylite and alteration products where those are exposed to meteoric water (Moore 1973).

Assemblage II was formed under a non-oxidizing condition, because all secondary phosphate minerals replacing primary triphylite are reduced species. The monocrystalline masses of triphylite are mostly corroded by vivianite, which also invaded the orthogonal cleavage planes and the cracks of triphylite. However, some other species, like whiteite, metaswitzerite, fairfieldite, eosphorite, ludlamite, messelite, and xanthoxenite, may be associated with vivianite, but are very fine grained. There must have been an increase in Ca activity during the weathering stage in order to form phosphates such as fairfieldite, messelite and xanthoxenite (Moore 1971, 1973, Fransolet 1975).

TABLE 6. TRACE-ELEMENT CONTENT OF SILICATES FROM VARIOUS ZONES OF THE SAPUCAIA PEGMATITE, MINAS GERAIS, BRAZIL

Mineral, sample	V	Cr	Zn	Ni	Ga	Rb	Sr	Nb	Pb
Muscovite, Sap-1	25	0	96	8	57	601	4	49	0
Muscovite, Sap-3	22	0	57	5	63	632	3	51	0
Muscovite, Sap-4	22	0	65	19	76	876	5	62	0
Muscovite, Sap-6	20	0	44	2	54	428	7	40	7
Muscovite, Sap-7	20	0	56	11	62	657	3	50	0
Muscovite, Sap-8	19	0	73	20	77	899	4	63	0
Muscovite, Sap-9	22	0	189	62	86	1571	4	80	0
Muscovite, Sap-11	20	0	50	10	66	681	3	54	0
Biotite, Sap-6	41	1	631	45	36	904	4	92	0
Schorl, Sap-1	4	180	666	0	42	0	4	0	0
Schorl, Sap-3	3	106	546	0	41	0	3	0	0
Schorl, Sap-4	6	169	1249	0	55	0	1	0	0
Schorl, Sap-7	4	152	1236	0	55	0	2	0	0
Schorl, Sap-10	7	100	1289	0	52	0	3	0	0
Schorl, Sap-11	4	107	1365	0	54	0	3	0	0
K-feldspar, Sap-1	16	67	7	0	8	1	16	0	77
K-feldspar, Sap-6	11	0	4	0	2	304	81	0	254
K-feldspar, Sap-7	15	50	15	0	6	8	13	0	67
K-feldspar, Sap-11	12	51	5	0	7	0	26	0	254
Albite, Sap-4	19	69	8	0	7	1	8	0	108
Albite, Sap-8	19	80	5	0	6	115	6	0	0
Albite, Sap-9	15	55	9	0	11	5	5	0	57
Albite, Sap-10	16	93	4	0	10	4	4	0	51
Beryl, Sap-4	16	73	117	0	6	27	4	0	0
Beryl, Sap-7	16	120	105	0	3	20	3	0	0
Beryl, Sap-11	12	113	82	0	8	27	5	0	0

Concentrations of the trace elements (in ppm) were obtained by X-ray-fluorescence measurements; 0: below the detection limit.

Interpretation of unusual petrographic textures involving phosphates and silicates

In assemblage I, interesting rims were observed around minerals associated with albite (Figs. 5a, c, d). The rim constituted by an intimate intergrowth of montebrasite + quartz, as well as the garnet rim, both reflect a reaction between phosphate minerals and feldspar during the albitization stage. This idea was first suggested by Hatert *et al.* (2010) to explain a rim of qingheite-(Fe²⁺) occurring around frondelite. The montebrasite + quartz assemblage (Fig. 5a) was formed according to the following process: during the albitization stage, triphylite oxidized to ferrisicklerite, and a significant amount of Li was leached out of the triphylite structure. This available Li, as well as some phosphorus from triphylite, then reacted with albite according to the reaction: triphylite + albite → ferrisicklerite + montebrasite + quartz. Frondelite replaced ferrisicklerite later, probably during the hydration stage. The excess sodium was certainly removed from the system by hydrothermal solutions because no lacroixite, NaAl(PO₄)F, was observed in the montebrasite + albite intergrowth.

The garnet and quartz rims, similar to those observed in metamorphic rocks (Joesten 1977, Ashworth & Birdi 1990, Ashworth *et al.* 1992, Attoh 1998), occur between

albite and frondelite (Fig. 5c), and can be explained by the reaction $\text{triphylite} + \text{albite} \rightarrow \text{almandine} + \text{quartz}$, followed by $\text{triphylite} \rightarrow \text{ferrisicklerite} \rightarrow \text{frondelite}$. The absence of diffusion profiles in garnet indicates that the mechanism responsible for this unusual petrographic texture is not a diffusion process but could be a dissolution–precipitation process, which Putnis & Austrheim (2010) invoked to explain the formation of sapphirine–plagioclase symplectite between garnet and kyanite in an eclogite. In such processes, the fluid phase plays a catalyst role only, and its chemical composition does not necessarily influence the compositions of reactants and products (Putnis & Austrheim 2010).

Finally, it is noteworthy that these reactions between phosphates and silicates can be used to constrain the position of phosphates in the genetic sequence. For example, the formation of a montebrasite rim necessitates the presence of Li in the reacting phosphate, which could have been provided by triphylite or ferrisicklerite. The absence of Li in heterosite indicates that this phosphate did not react with albite to form montebrasite, and that its position in the genetic sequence must come after the metasomatic albitization stage.

Geochemical evolution of minerals and pegmatite differentiation

The $\text{Fe}/(\text{Fe} + \text{Mn})$ value in primary triphylite is commonly used to estimate the degree of differentiation of granitic pegmatites (Keller *et al.* 1994a, 1994b, Franolet *et al.* 1986, Roda *et al.* 2004, Roda-Robles *et al.* 2005, 2010, Vignola *et al.* 2008). As already observed in the literature (Mason 1941, Fontan *et al.* 1976, Franolet *et al.* 1986, Franolet 2007, Vignola *et al.* 2008), the Fe, Mn, and Mg contents of phosphates do not show significant variations during the “Quensel–Mason” oxidation sequence. This finding is confirmed by the electron-microprobe analyses performed on phosphates from Sapucaia (Fig. 4), and as a consequence, we can also use the $\text{Fe}/(\text{Fe} + \text{Mn})$ and $\text{Mg}/(\text{Fe} + \text{Mn} + \text{Mg})$ values in ferrisicklerite and heterosite to estimate the degree of differentiation of the different zones in the Sapucaia pegmatite. The samples investigated herein show a clear decrease in the $\text{Fe}/(\text{Fe} + \text{Mn})$, from 0.75 in sample Sap–1, to 0.71 in sample Sap–4 (Fig. 4), whereas $\text{Mg}/(\text{Fe} + \text{Mn} + \text{Mg})$ also shows this decrease, from 0.19 in sample Sap–1, to 0.13 in sample Sap–4 (Fig. 4, Table 2). These chemical variations are correlated with the degree of differentiation, which changes from the border to the center of the pegmatite: phosphates from the differentiated inner zone, in which sample Sap–4 is located, show low Fe and Mg contents if compared with the less differentiated phosphates from the outer zone, where samples Sap–1 and Sap–7b were collected. These observations are in good agreement with the geochemical evolution of pegmatites described by Ginsburg (1960) and Simmons & Webber (2008). Sample Sap–6b was not found in place, but its chemical

composition suggests that its degree of evolution is similar to that of sample Sap–1 (Fig. 4). Moreover, the Mn-rich triphylite from samples Prb–1b, Sap–12a, and Sap–12d, which are not located on the map, certainly corresponds to a second generation of triphylite, which crystallized at lower temperatures (Fig. 4).

The trace elements and the major elements in silicates follow the same geochemical trend as phosphate minerals. In muscovite, we observe a substitution $3(\text{Mg},\text{Fe})^{2+} = 2\text{Al}^{3+} + \square$, which leads to an increase in Al from the EWZ to IZ of the pegmatite (Fig. 8). Moreover, the K/Rb value also decreases, whereas Ga and Nb increase from the EWZ to the pegmatite core (Fig. 8). These trends confirm the geochemical evolution generally observed in granitic pegmatites (Ginsburg 1960, Simmons & Webber 2008).

In tourmaline, the dominant substitution from the EWZ to the IZ is Mg for Fe^{2+} , as observed in several pegmatites (Roda-Robles *et al.* 2004, 2011, Gadas *et al.* 2011). As a consequence, differentiation results in an increase in the schorl component and a decrease in the dravite component in tourmaline. This substitution is generally coupled with a $\text{Na} + \text{Fe}^{2+} = \square + \text{Al}^{3+}$ substitution mechanism, which corresponds to the schorl–foitite series (Selway *et al.* 1999, 2000, Tindle *et al.* 2002, Roda-Robles *et al.* 2004, 2011). At Sapucaia, the schorl–dravite substitution is evident, and evolution of chemical compositions along this solid solution follows the differentiation trends observed in the literature (Fig. 9). However, no satisfactory correlation has been observed between the zones of the Sapucaia pegmatite and the compositions of tourmaline along the schorl–foitite and schorl–elbaite series.

The presence of Mn-bearing almandine in the IWZ is another line of evidence that indicates the limited degree of evolution of this zone, compared to the IZ, where garnet does not appear (Černý & Hawthorne 1982, Whitworth 1992). From a more general point of view, the dominance of Fe over Mn in garnet and in phosphate minerals, the high Mg content in triphylite, as well as the low amounts of trace elements in silicates, indicate that the Sapucaia pegmatite is a poorly fractionated and geochemically primitive LCT-type pegmatite (Franolet *et al.* 1986, Roda *et al.* 2004, Vignola *et al.* 2008).

ACKNOWLEDGEMENTS

Many thanks are due to E. Grew, D. London, R.F. Martin, as well as to an anonymous reviewer, for their constructive comments on the manuscript. Jacques Cassedanne is acknowledged for his help during the field trip in Brazil, F.H. thanks the FRS–F.N.R.S. (Belgium) for a position of “Chercheur qualifié”, and M.B. thanks the FNR (Luxembourg) for Ph.D. grant EXT–BFR07–137 TR. This paper is dedicated to Petr Černý, for his outstanding contribution to pegmatology, especially in the field of phosphate mineralogy.

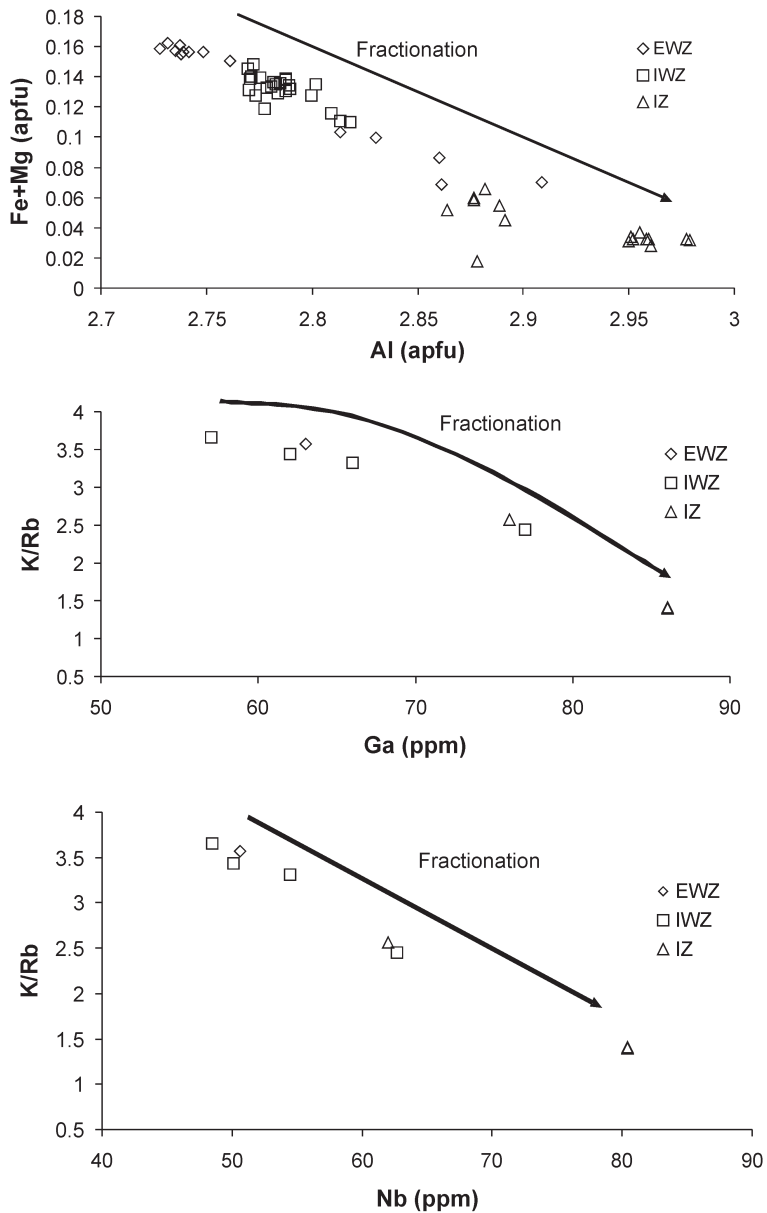


FIG. 8. Plots of Fe + Mg versus Al, K/Rb versus Ga, and K/Rb versus Nb showing the geochemical evolution of muscovite from the EWZ to the IZ, at Sapucaia.

REFERENCES

- ALFONSO, P., MELGAREJO, J.C., YUSTA, I. & VELASCO, F. (2003): Geochemistry of feldspars and muscovite in granitic pegmatite from the Cap de Creus field, Catalonia, Spain. *Can. Mineral.* **41**, 103-116.
- ANDERSON, S.D., ČERNÝ, P., HALDEN, N.M., CHAPMAN, R. & UHER, P. (1998): The Yitt-B pegmatite swarm at Bernic Lake, southeastern Manitoba: a geochemical and paragenetic anomaly. *Can. Mineral.* **36**, 283-301.

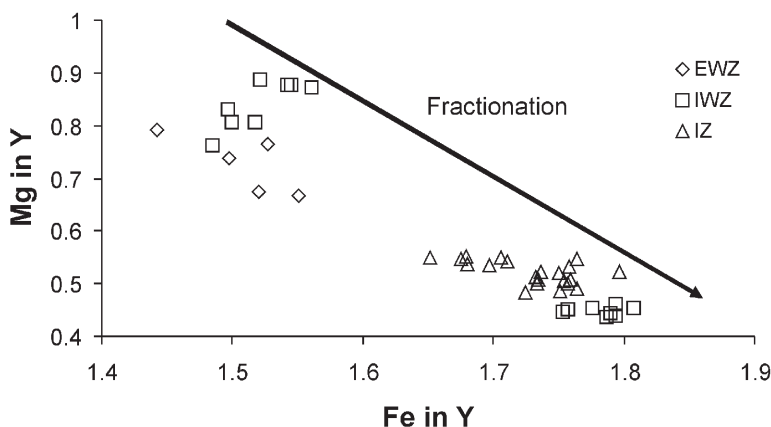


FIG. 9. A Mg versus Fe diagram showing the schorl–dravite substitution from the EWZ to the IZ, at Sapucaia.

- ARIMA, M. & YAMASHITA, H. (1994): P_2O_5 -rich garnet from Hosokawa-dani, Tanzawa Mountain-land. *J. Mineral. Petrol. Econ. Geol.* **89**, 166.
- ARREDONDO, E.H., ROSSMAN, G.R. & LUMPKIN, G.R. (2001): Hydrogen in spessartine–almandine garnets as a tracer of granitic pegmatite evolution. *Am. Mineral.* **86**, 485-490.
- ASHWORTH, J.R. & BIRDI, J.J. (1990): Diffusion modelling of coronas around olivine in an open system. *Geochim. Cosmochim. Acta* **54**, 2389-2401.
- ASHWORTH, J.R., BIRDI, J.J. & EMMET, T.F. (1992): Diffusion in coronas around clinopyroxene: modelling with local equilibrium and steady state, and non-steady-state modification to account for zoned actinolite–hornblende. *Contrib. Mineral. Petrol.* **109**, 307-325.
- ATENCIO, D., CHUKANOV, N.V., COUTINHO, J.M.V., MENEZES FILHO, L.A.D., DUBINCHUK, V.T. & MÖCKEL, S. (2007): Ruifrancoite, a new Fe^{3+} -dominant monoclinic member of the roscherite group from Galiléia, Minas Gerais, Brazil. *Can. Mineral.* **45**, 1263-1273.
- ATTOH, K. (1998): Models for orthopyroxene–plagioclase and other corona reactions in metanorites, Dahomeyide orogen, West Africa. *J. Metam. Geol.* **16**, 345-362.
- BILAL, E., HORN A.H., NALINI, H.A., JR., MELLO, F.M., CORREIA-NEVES, J.M., GIRET, A.R., MOUTTE, J., FUZIKAWA, K. & FERNANDES, M.L.S. (2000): Neoproterozoic granitoid suites in southeastern Brazil. *Revista Brasileira de Geociências* **30**, 51-54.
- BILAL, E., NALINI, H.A., HORN, A.H., CORREIA-NEVES, J.M., GIRET, A.R., FUZIKAWA, K., FERNANDES, M.L.S., MELLO, F. & MOUTTE, J. (1998): Neoproterozoic granitoid suites of Rio Doce Region, Brazil. *Int. Conf. on Precambrian and Craton Tectonics (Ouro Preto), Extended Abstr.*, 41-43.
- BREITER, K. & KOLLER, F. (2003): Phosphorus-rich garnets from leucocratic igneous rocks (Přibyslavice, Moldanubicum, Czech Republic). *Mitt. Österr. Mineral. Ges.* **148**, 97-98.
- BREITER, K., NOVÁK, M., KOLLER, F. & CEMPÍREK, J. (2005): Phosphorus – an omnipresent minor element in garnet of diverse textural types from leucocratic granitic rocks. *Mineral. Petrol.* **85**, 205-221.
- BURNHAM, C.W. (1991): *LCLSQ version 8.4, least-squares refinement of crystallographic lattice parameters*. Dept. of Earth & Planetary Sciences, Harvard University, Cambridge, Massachusetts.
- BURNS, P.C., MACDONALD, D.J. & HAWTHORNE, F.C. (1994): The crystal chemistry of manganese-bearing elbaite. *Can. Mineral.* **32**, 31-41.
- BURT, D.M. (1996): Compositional limits of phosphorus substitution in garnet in pegmatites and in the mantle. *Geol. Assoc. Can. – Mineral. Assoc. Can., Program Abstr.* **2**, A-15.
- CASSEDANNE, J. & BAPTISTA, A. (1999): The Sapucaia pegmatite, Minas Gerais, Brazil. *Mineral. Rec.* **30**, 361-366.
- CASSEDANNE, J.P. & CASSEDANNE, J.O. (1985): Découverte d'un phosphate métamictite dans la pegmatite du Sapucaia (Minas Gerais). *Anais da Academia Brasileira de Ciências* **57**, 325-327.
- ČERNÝ, P. & HAWTHORNE, F.C. (1982): Selected peraluminous minerals. In *Granitic Pegmatites in Science and Industry* (P. Černý, ed.). *Mineral. Assoc. Can., Short-Course Handbook* **8**, 163-186.
- CHAPMAN, C.A. (1943): Large magnesia-rich triphylite crystals in pegmatites. *Am. Mineral.* **28**, 90-98.

- CHAVES, M.L. & SCHOLZ, R. (2008): Pegmatito Gentil (Mendes Pimentel, MG) e suas paragêneses mineralógicas de fosfatos raros. *R. Esc. Minas, Ouro Preto, Geociências* **61**(2), 141-149.
- CHAVES, M.L., SCHOLZ, R., ATENCIO, D. & KARFUNKEL, J. (2005): Assembléias e paragêneses minerais singulares nos pegmatitos de região de Galiléia (Minas Gerais). *Geociências* **24**(2), 143- 161.
- CHESNOKOV, B.V., VILISOV, V.A., POLYAKOV, V.O. & BUSHMAKIN, A.F. (1989): New phosphates from the Ilmeny Reserve. In *Minerals and Mineral Resources of Mining Regions of the Urals*, 3-10 (in Russian).
- CHOPIN, C., OBERTI, R. & CÂMARA, F. (2006): The arrojadite enigma. II. Compositional space, new members, and nomenclature of the group. *Am. Mineral.* **91**, 1260-1270.
- CORBELLÀ, M. & MELGAREJO, J.C. (1990): Características y distribución de los fosfatos de las pegmatitas graníticas de la península de Cap de Creus (Pirineo oriental Catalan). *Bol. Soc. Esp. Mineral.* **13**, 169-182.
- CORREIA NEVES, J.M., PEDROSA SOARES, A.C., MARCIANO, V.R.P.D.R. (1986): A provincial pegmatítica oriental do Brasil à luz dos conhecimentos atuais. *Revista Brasileira de Geociências* **16**,106-118.
- COZZUPOLI, D., GRUBESSI, O., MOTTANA, A. & ZANAZZI, P.F. (1987): Cyrilovite from Italy: structure and crystal chemistry. *Mineral. Petrol.* **37**, 1-14.
- FARIAS, C.C. (1976): *Mineralogia do Pegmatito Alto Boqueirão, Parelhas-RN*. Ph.D. thesis, Universidade Federal de Pernambuco, Recife, Brazil.
- FONTAN, F., HUVELIN, P., ORLIAC, M. & PERMINGEAT, F. (1976): La ferrisicklerite des pegmatites de Sidi-bou-Othmane (Jebilet, Maroc) et le groupe des minéraux à structure de triphylite. *Bull. Soc. fr. Minéral. Cristallogr.* **99**, 274-286.
- FRANSOLET, A.-M. (1975): *Etude minéralogique et pétrologique des phosphates de pegmatites granitiques*. Ph.D. thesis, Université de Liège, Liège, Belgium.
- FRANSOLET, A.-M. (1976): L'huréalite: ses propriétés minéralogiques et son rôle dans l'évolution génétique des phases Li(Fe,Mn)PO₄. *Bull. Soc. fr. Minéral. Cristallogr.* **99**, 261-273.
- FRANSOLET, A.-M. (1980): The eosphorite–childrenite series associated with the Li–Mn–Fe phosphate minerals from the Buranga pegmatite, Rwanda. *Mineral. Mag.* **43**, 1015-1023.
- FRANSOLET, A.-M. (2007): Phosphate associations in the granitic pegmatites: the relevant significance of these accessory minerals. *Granitic pegmatites: The state of the Art, International symposium, Porto, Portugal. Abstr. Vol.*, 7-8.
- FRANSOLET, A.-M., ABRAHAM, K. & SPEETJENS, J.-M. (1985): Evolution génétique et signification des associations de phosphates de la pegmatite d'Angarf-Sud, plaine de Tazenakht, Anti-Atlas, Maroc. *Bull. Minéral.* **108**, 551-574.
- FRANSOLET, A.-M., ANTENUCCI, D., SPEETJENS, J.-M. & TARTE, P. (1984): An X-ray determinative method for the divalent cation ratio in the triphylite–lithiophilite series. *Mineral. Mag.* **48**, 373-381.
- FRANSOLET, A.-M., KELLER, P. & FONTAN, F. (1986): The phosphate mineral associations of the Tsaobismund pegmatite, Namibia. *Contrib. Mineral. Petrol.* **92**, 502-517.
- GADAS, P., NOVÁK, M., FILIP J. & STANĚK, J. (2011). Zoned foitite → schorl → dravite → magnesiofoitite crystals from pockets in anatectic pegmatites of Moldanubian zone, Czech Republic. *Geológica Argentina, Serie D, Publicación Especial* **14**, 87-89.
- GINSBURG, A.I. (1960): Specific geochemical features of the pegmatitic process. *Proc. 21st Int. Geol. Congress (Norden)* **17**, 111-121.
- HATERT, F., BAIJOT, M., PHILIPPO, S. & WOUTERS, J. (2010): Qingheite-(Fe²⁺), Na₂Fe²⁺MgAl(PO₄)₃, a new phosphate mineral from Sebastião Cristino pegmatite, Minas Gerais, Brazil. *Eur. J. Mineral.* **22**, 459-467.
- HATERT, F., OTTOLINI, L., FONTAN, F., KELLER, P., RODA-ROBLES, E. & FRANSOLET, A.-M. (2011): The crystal chemistry of olivine-type phosphates. *Geológica Argentina, Serie D, Publicación Especial* **14**, 103-105.
- HIRSON, J.R. (1965): Nota sobre os fosfatos de Sapucaia. *Anais da Academia Brasileira de Ciências* **40**, 471-475.
- HORVATH, M. & ATENCIO, D. (1998): Robertsita, mitridatita e cacoxenita no Pegmatito Sapucaia, Galiléia, MG. *Congresso Brasileiro de Geologia, 40, Belo Horizonte, Anais*, 296.
- JOESTEN, R. (1977): Evolution of mineral assemblage zoning in diffusion metasomatism. *Geochim. Cosmochim. Acta* **41**, 649-670.
- KAMPF, A.R., STEELE, I.M. & LOOMIS, T.A. (2008): Jahnsite-(NaFeMg), a new mineral from the Tip Top mine, Custer County, South Dakota: description and crystal structure. *Am. Mineral.* **93**, 940-945.
- KELLER, P. (1988): Dendritic phosphate minerals and their paragenetic relation to the silicate minerals of pegmatites from Namibia and from the Black Hills, South Dakota, U.S.A. *Neues Jahrb. Mineral., Abh.* **159**, 249-281.
- KELLER, P., FONTAN, F. & FRANSOLET, A.-M. (1994b): Inter-crystalline cation partitioning between minerals of the triplite – zwieselite – magniotriplite and the triphylite – lithiophilite series in granitic pegmatites. *Contrib. Mineral. Petrol.* **118**, 239-248.
- KELLER, P., FRANSOLET, A.-M. & FONTAN, F. (1994a): Triphylite–lithiophilite and triplite–zwieselite in granitic pegmatites: their textures and genetic relationships. *Neues Jahrb. Mineral., Abh.* **168**, 127-145.

- KELLER, P. & VON KNORRING, O. (1989): Pegmatites at the Okatjimukuju farm. Karibib, Namibia. I. Phosphate mineral associations of the Clementine II pegmatite. *Eur. J. Mineral.* **1**, 567-593.
- LINDBERG, M.L. (1949): Frondelite and the frondelite-rock-bridgeite series. *Am. Mineral.* **34**, 541-549.
- LINDBERG, M.L. (1957): Relationship of the minerals avelinoite, cyrilovite, wardite. *Am. Mineral.* **42**, 204-213.
- LINDBERG, M.L. (1962): Manganian lipscombite from the Sapucaia pegmatite mine, Minas Gerais, Brazil, first occurrence of lipscombite in nature. *Am. Mineral.* **47**, 353-359.
- LINDBERG, M.L. & MURATA, K.J. (1952): Minerals of Sapucaia pegmatite mine, faheyite, a new beryllium phosphate. *Geol. Soc. Am., Bull.* **63**, 1275-1276 (abstr.).
- LINDBERG, M.L. & MURATA, K.J. (1953): Faheyite, a new phosphate mineral from Sapucaia pegmatite mine, Minas Gerais, Brazil. *Am. Mineral.* **38**, 263-270.
- LINDBERG, M.L. & PECORA, W.T. (1954a): Avelinoite, a new hydrous sodium phosphate mineral from Minas Gerais, Brazil. *Science* **120**, 1074-1075.
- LINDBERG, M.L. & PECORA, W.T. (1954b): Tavorite and barbosalite: two new phosphate minerals from Minas Gerais, Brazil. *Science* **119**, 739.
- LINDBERG, M.L. & PECORA, W.T. (1955): Tavorite and barbosalite: two new phosphate minerals from Minas Gerais, Brazil. *Am. Mineral.* **119**, 952-966.
- LINDBERG, M.L. & PECORA, W.T. (1958): Phosphate minerals from Sapucaia pegmatite mine, Minas Gerais. *Boletim da Sociedade Brasileira de Geologia* **7**(2), 5-14.
- LINDBERG, M.L., PECORA, W.T., & BARBOSA, A.L.M. (1953): Moraesite, a new hydrous beryllium phosphate from Minas Gerais, Brazil. *Am. Mineral.* **38**, 1126-1133.
- LONDON, D., WOLF, M.B., MORGAN, G.B., VI & GALLEGO GARRIDO, M. (1999): Experimental silicate-phosphate equilibria in peraluminous granitic magmas, with a case study of the Albuquerque batholith at Tres Arroyos, Badajoz, Spain. *J. Petrol.* **40**, 215-240.
- LOSEY, A., RAKOVAN, J., HUGHES, J.M., FRANCIS, C.A. & DYAR, M.D. (2004): Structural variation in the lithiophilite-triphylite series and other olivine-group structures. *Can. Mineral.* **42**, 1105-1115.
- MASON, B. (1941): Minerals of the Varutråsk pegmatite. XXIII. Some iron-manganese phosphate minerals and their alteration products, with special reference to material from Varutråsk. *Geol.Fören. Stockholm Förh.* **63**, 117-175.
- MOORE, P.B. (1971): The $\text{Fe}^{2+}_3(\text{H}_2\text{O})_n(\text{PO}_4)_2$ homologous series: crystal chemical relationships and oxidized equivalents. *Am. Mineral.* **56**, 1-17.
- MOORE, P.B. (1973): Pegmatites phosphates: descriptive mineralogy and crystal chemistry. *Mineral. Rec.* **4**, 103-130.
- MOORE, P.B. (1982): Pegmatite minerals of P(V) and B(III). In *Granitic Pegmatites in Science and Industry* (P. Černý, ed.). *Mineral. Assoc. Can., Short Course Handbook* **8**, 267-291.
- MOORE, P.B. & ARAKI, T. (1974): Jahnsite, $\text{CaMn}^{2+}\text{Mg}_2(\text{H}_2\text{O})_8\text{Fe}^{3+}_2(\text{OH})_2[\text{PO}_4]_4$: a novel of stereoisomerism of ligands about octahedral corner-chains. *Am. Mineral.* **59**, 964-973.
- MOORE, P.B. & ITO, J. (1978): I. Whiteite, a new species, and a proposed nomenclature for jahnsite-whiteite complex series. II. New data on xanthoxenite. III. Salmonsite discredited. *Mineral. Mag.* **42**, 309-323.
- MOORE, P.B. & MOLIN-CASE, J. (1974): Contribution to pegmatite phosphate giant crystal paragenesis. II. The crystal chemistry of wyllieite, $\text{Na}_2\text{Fe}^{2+}_2\text{Al}(\text{PO}_4)_3$, a primary phase. *Am. Mineral.* **59**, 280-290.
- MORTEANI, G., PREINFALK, C. & HORN, A.H. (2000): Classification and mineralization potential of the pegmatites of the Eastern Brazilian Pegmatite Province. *Mineral. Deposita* **35**, 638-655.
- NALINI, H.A. (1997): *Caractérisation des suites magmatiques néoprotérozoïques de la région de Conselheiro Pena et Galiléia (Minas Gerais, Brésil): étude géochimique et structurale des suites de Galiléia et Urucum et leur relation avec les pegmatites à éléments rares associées*. Ph.D. thesis, Ecole des mines de Saint Etienne et Ecole des mines de Paris, France.
- NALINI, H.A., BILAL, E., PAQUETTE, J.-L., PIN, C. & RÔMULO, M. (2000): Géochronologie U-Pb et géochimie isotopique Sr-Nd des granitoïdes néoprotérozoïques des suites Galiléia et Urucum, vallée du Rio Doce, Sud-Est du Brésil. *C.R. Acad. Sci., Sci. de la Terre et des Planètes* **331**, 459-466.
- PAIVA, G. de (1946): Província pegmatíficas do Brazil. *Boletim DNPM-DFMP* **78**, 13-21.
- PECORA, W.T., KEPPLER, M.R., LARRABEE, D.M., BARBOSA, A.L.M. & FRAYHA, R. (1950): Mica deposits in Minas Gerais, Brazil. *U.S. Geol. Surv. Bull.* **964-C**, 205-305.
- PEDROSA-SOARES, A.C., CHAVES, M. & SCHOLZ, R. (2009): Eastern Brazilian pegmatite province. *4th Int. Symp. on Granitic Pegmatites, Field trip guide*, 1-28.
- PEDROSA-SOARES, A.C., DE CAMPOS, C.P., NOCE, C.M., SILVA, L.C., NOVO, T., RONCATO, J., MEDEIROS, S., CASTAÑEDA, C., QUEIROGA, G., DANTAS, E., DUSSIN, I. & ALKIMM, F. (2011): Late Neoproterozoic – Cambrian granitic magmatism in the Araçuaí orogen (Brazil), the Eastern Brazilian Pegmatite Province and related mineral resources. In *Granite-Related Ore Deposits* (A.N. Sial, J.S. Bettencourt, C.P. De Campos & V.P. Ferreira, eds.). *Geol. Soc., Spec. Publ.* **350**, 25-51.
- PEDROSA-SOARES, A.C., NOCE, C.M., WIEDEMANN, C.M. & PINTO, C.P. (2001): The Araçuaí – West-Congo orogen in Brazil: an overview of confined orogen formed during Gondwanaland assembly. *Precamb. Res.* **110**, 307-323.

- PUTNIS, A. & AUSTRHEIM, H. (2010): Fluid-induced processes: metasomatism and metamorphism. *Geofluids* **10**, 254-269.
- PUTZER, H. (1976): *Metallogenetische Provinzen in Südamerika*. Schweizerbart'sche Verlagsbuchhandlung, Stuttgart, Germany.
- QUENSEL, P. (1937). Minerals of the Varuträsk pegmatite. I. The lithium–manganese phosphates. *Geol. Fören. Stockholm Förh.* **59**, 77-96.
- QUENSEL, P. (1957). The paragenesis of the Varuträsk pegmatite, including a review of its mineral assemblage. *Arkiv Mineral. Geol.* **2**(2), 9-125.
- RASTSVETAEVA, R.K., CHUKANOV, N.V. & VERIN, I.A. (2005): Crystal structure of roschelite. *Dokl. Akad. Nauk* **403**(6), 768-771 (in Russ.), *Dokl. Chem.* **403**(2), 160-163.
- REDHAMMER, G.J., ROTH, G., TIPPETT, G., BERNROIDER, M., LOTTERMOSER, W., AMTHAUER, G. & HOCHLEITNER, R. (2006): Manganian rockbridgeite $\text{Fe}_{4.32}\text{Mn}_{0.62}\text{Zn}_{0.06}(\text{PO}_4)_3(\text{OH})_5$: structure analysis and ^{57}Fe Mössbauer spectroscopy. *Acta Crystallogr.* **C62**, i24-i28.
- RODA, E., FONTAN, F., PESQUERA, A., VELASCO, F. (1996): The phosphate mineral association of the granitic pegmatites of the Fregeneda area (Salamanca, Spain). *Mineral. Mag.* **60**, 767-778.
- RODA, E., PESQUERA, A., FONTAN, F. & KELLER, P. (2004): Phosphate mineral associations in Cañada pegmatite (Salamanca, Spain): paragenetic relationships, chemical compositions, and implications for pegmatite evolution. *Am. Mineral.* **89**, 110-125.
- RODA, E., PESQUERA, A., VELASCO, F. & FONTAN, F. (1999): The granitic pegmatites of the Fregeneda area (Salamanca, Spain): characteristics and petrogenesis. *Mineral. Mag.* **63**, 535-558.
- RODA-ROBLES, E., FONTAN, F., PESQUERA PÉREZ, A. & KELLER, P. (1998). The Fe–Mn phosphate associations from the Pinilla de Fermoselle pegmatite, Zamora, Spain: occurrence of kryzhanovskite and natrodufrénite. *Eur. J. Mineral.* **10**, 155-167.
- RODA-ROBLES, E., PESQUERA, A., GIL-CRESPO, P.P., TORRES-RUIZ, J. & FONTAN, F. (2004): Tourmaline from the rare element Pinilla pegmatite, (Central Iberian Zone, Zamora, Spain): chemical variation and implications for pegmatitic evolution. *Mineral. Petrol.* **81**, 249-263.
- RODA-ROBLES, E., PESQUERA, A., GIL, P.P., TORRES-RUIZ, J. & FONTAN, F. (2005): Origin and internal evolution of the Li–F–Be–B–P-bearing Pinilla de Fermoselle pegmatite (Central Iberian Zone, Zamora, Spain). *Am. Mineral.* **90**, 1887-1899.
- RODA-ROBLES, E., SIMMONS, W., NIZAMOFF, J., PESQUERA, A., GIL-CRESPO, P.P. & TORRES-RUIZ, J. (2011): Chemical variation in tourmaline from the Berry–Havey pegmatite (Maine, USA), and implications for pegmatite evolution. *Geológica Argentina, Serie D, Publicación Especial* **14**, 165-168.
- RODA-ROBLES, E., VIEIRA, R., PESQUERA, A. & LIMA, A. (2010): Chemical variations and significance of phosphates from the Fregeneda–Almendra pegmatite field, Central Iberian Zone (Spain and Portugal). *Mineral. Petrol.* **100**, 24-34.
- SELWAY, J.B., ČERNÝ, P., HAWTHORNE, F.C. & NOVÁK, M. (2000): The Tanco pegmatite at Bernic lake, Manitoba. XIV. Internal tourmaline. *Can. Mineral.* **38**, 877-891.
- SELWAY, J.B., NOVÁK, M., ČERNÝ, P. & HAWTHORNE, F.C. (1999): Compositional evolution of tourmaline in lepidolite-subtype pegmatites. *Eur. J. Mineral.* **11**, 569-584.
- SIMMONS, W.B. & WEBBER, K.L. (2008): Pegmatite genesis: state of the art. *Eur. J. Mineral.* **20**, 421-438.
- SVISERO, D.P. (1976): Ocorrência de herderita no pegmatito de Sapucaia, município de Galiléia, Minas Gerais, *Ciência e Cultura* **28**(7), 212.
- TARTE, P., FRANSOLETT, A.-M. & PILLARD, F. (1984). Le spectre infrarouge de la cyrilovite et de la wardite: corrélations entre la structure et la composition chimique. *Bull. Minéral.* **107**, 745-754.
- TAYLOR, L.S. & WISE, M.A. (1995): Geochemistry and mode of occurrence of phosphorus in spessartine. *Geol. Soc. Am., Abstr. Programs* **27**, A470.
- TAYLOR, L.S., WISE, M.A., SIMMONS, W.B. & FALSTER, A.U. (1997): Occurrence of phosphorus in garnets from gem-bearing pegmatite. *Rock & Minerals* **72**, 189-190.
- TINDLE, A.G., BREAKS, F.W. & SELWAY, J.B. (2002): Tourmaline in petalite-subtype granitic pegmatites: evidence of fractionation and contamination from the Pakeagama Lake and Separation Lake areas of northwestern Ontario, Canada. *Can. Mineral.* **38**, 877-891.
- VIANA, R.R., JORDT-EVANGELISTA, H. & STERN, W.B. (2007): Geochemistry of muscovite from pegmatites of the Eastern Brazilian Pegmatite Province: a clue to petrogenesis and mineralization potential. *Eur. J. Mineral.* **19**, 745-755.
- VIGNOLA, P., DIELLA, V., OPPICCI, P., TIEPOLO, M. & WEISS, S. (2008): Phosphate assemblages from the Brissago granitic pegmatite, western Southern Alps, Switzerland. *Can. Mineral.* **46**, 635-650.
- WHITWORTH, M.P. (1992): Petrogenetic implications of garnets associated to lithium pegmatites from SE Ireland. *Mineral. Mag.* **56**, 75-83.
- ZHANG, C., GIERÉ, R., STÜNITZ, H., BRACK, P. & ULMER, P. (2001): Garnet–quartz intergrowths in granitic pegmatites from Bergell and Adamello, Italy. *Schweiz. Mineral. Petrogr. Mitt.* **81**, 89-113.

Received July 12, 2011, revised manuscript accepted November 22, 2012.